




A review of carbon-based magnetic microwave-absorbing composites with one-dimensional structure

Zhengguo Jiao¹, Mingliang Ma^{1,*} , Yuxin Bi¹, Chenggang Lu², Chao Feng¹, Ping Lyu¹, Jindi Zhao¹, and Yong Ma^{3,*}

¹School of Civil Engineering, Qingdao University of Technology, Qingdao 266033, People's Republic of China

²School of Environmental and Municipal Engineering, Qingdao University of Technology, Qingdao 266033, People's Republic of China

³School of Material Science and Engineering, Shandong University of Science and Technology, Qingdao 266590, People's Republic of China

Received: 1 June 2022

Accepted: 23 September 2022

Published online:
12 October 2022

© The Author(s), under exclusive licence to Springer Science+Business Media, LLC, part of Springer Nature 2022

ABSTRACT

With the development of information technology, the problem of electromagnetic pollution was increasingly prominent. At present, it had brought serious harm to electronic equipment and biology. Microwave absorption (MA) materials were the key to solve this problem. One-dimensional (1D) carbon-based magnetic composites were prepared by compounding with carbon materials, which improved the deficiency of ferromagnetic MA materials. In this review, the unique advantages of 1D carbon-based magnetic composites were discussed in detail. Firstly, the preparation methods of carbon fibers with different structures were reviewed, including the important roles of these structures in MA. After that, the properties of carbon nanotubes (CNTs) combined with different magnetic materials were introduced. The biomass-derived 1D carbon materials possessed the unique structure, which was obtained difficultly by artificial ways. Their advantages and current progress for MA were analyzed in detail. Finally, according to the current development of MA materials, the challenges and research prospects of 1D carbon-based magnetic composites were discussed, and some suggestions were proposed as well.

Introduction

Due to the popularization of electronic equipment, computer network and mobile phone, electromagnetic wave became ubiquitous and brought a series of

problems inevitably [1–3]. For example, electromagnetic wave pollution would have detrimental effects on human health and precision instruments [4–11], so that the world health organization ranked it as the fourth pollution after water pollution, air pollution

Handling Editor: Kyle Brinkman.

Address correspondence to E-mail: mamingliang@qut.edu.cn; mayong@sdust.edu.cn

<https://doi.org/10.1007/s10853-022-07803-7>

and noise pollution [12–15]. MA materials could convert electromagnetic waves into joule heat to solve electromagnetic wave pollution [16]. At the same time, MA materials could also be used in the military anti-reconnaissance field to prevent the aircraft by enemy radars. Therefore, the research of MA materials had become a hotspot in recent years.

It was well known that electromagnetic wave was composed of oscillating electric and magnetic fields. Therefore, the loss of MA materials was mainly composed of dielectric loss and magnetic loss. The reflection loss (RL) values were calculated by the following equations at a given frequency and thickness layer according to the transmit line theory [17, 18]:

$$Z_{in} = Z_0 \sqrt{\frac{\mu_r}{\epsilon_r} \tanh \left[j \left(\frac{2\pi f d}{c} \right) \sqrt{\mu_r \epsilon_r} \right]}$$

$$RL(\text{dB}) = 20 \lg \left| \frac{Z_{in} - Z_0}{Z_{in} + Z_0} \right|$$

where Z_0 was the impedance of free space, Z_{in} was the input impedance of the absorber, c was the velocity of EM wave in free space, f was the frequency of electromagnetic wave, and d was the thickness of the absorber. Therefore, MA materials needed to achieve strong absorption of microwaves under the synergistic effect of dielectric and magnetic losses.

Common magnetic loss materials were mainly Fe [19], Co [20], Ni [21] and their compounds because of high saturation magnetization and high Snoek's limit²². Unfortunately, these conventional magnetic loss materials had high density and poor chemical resistance. Compared with magnetic loss materials, carbon materials had the advantages of low density, chemical corrosion resistance and good dielectric properties^{23, 24}. According to the expression of skin depth ($\delta = \sqrt{1/\pi\mu_0\mu_i\sigma f}$), the large conductivity of carbon would lead to low skin depth, so that most microwaves could not enter the interior of the MA materials²⁵. The researchers combined magnetic particles with carbon to improve MA capabilities. Magnetic materials could adjust the impedance matching of carbon materials and increase the phase interfaces. Furthermore, the carbon materials could enhance the chemical corrosion resistance of magnetic materials and reduce their density.

In addition to the composition of MA materials, the microstructure also deeply affected the properties of

MA materials. Among all kinds of structures, 1D structures had attracted much attention because of their unique shape anisotropy and spatial constraint effect. Moreover, 1D carbon nanofibers had the quantum size effect and macroscopic quantum tunneling effect, and the split energy level spacing was just within the energy range of microwave to increase the absorption pathway of microwave^{26–28}. The synergistic interaction between 1D materials and other structures (flower-like structure, core-shell structure and porous structure) could also further improve the microwave absorption performance. In addition, the preparation of 1D microwave absorption materials was also very convenient, and electrospinning and hydrothermal method were common preparation methods.

Due to the excellent properties of 1D carbon-based magnetic composites, the number of publications had increased significantly in the last five years, as shown in Fig. 1. Herein, the research progress of 1D carbon-based magnetic composites for MA was reviewed. The results showed that a reasonable microstructure could increase the interface polarization and microwave reflection. Next, 1D carbon-based magnetic composites with different structures were discussed to explore the influence of structure on MA properties. Meanwhile, challenges for the development of 1D carbon-based magnetic composites were pointed out to design better MA materials.

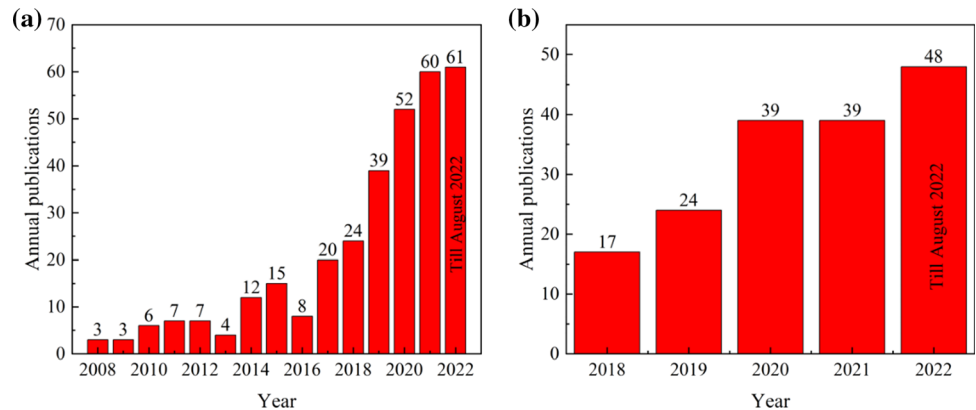
Magnetic carbon fiber composites

Carbon fibers were widely used in MA due to their high dielectric loss and low density²⁹. By combining carbon fibers with other magnetic loss materials, the composite absorbers would have complex interfaces and produce interfacial polarization to improve the MA performance³⁰. Through the modification of carbon fiber, the strong absorption of microwaves by 1D magnetic carbon materials was achieved. The structure of common 1D carbon fiber materials is shown in Fig. 2.

Porous composites

The porous MA materials could make the microwave reflect several times to extend the transmission path of microwaves within the material, thus accelerating the attenuation of microwaves. Proper porosity could

Figure 1 Number of the publications on **a** “MA” and “1D or nanofibers or nanochain or nanowire” and “Fe or Co or Ni” **b** “MA and carbon” and “1D or nanofibers or nanochain or nanowire” and “Fe or Co or Ni” searched by Web of Science.



improve the impedance matching and reduce the dielectric constant and the density of MA materials [35]. In addition, a higher gas–solid interface enhanced the interfacial polarization of MA materials and then improves the attenuation ability of microwaves.

With the increase in the papers on porous carbon fiber, various preparation methods of porous carbon fiber were reported [36–38]. Hard template method was often used for the preparation of macroporous carbon fibers. Liu et al. [39, 40] used SiO₂ as a template to prepare 1D materials by electrospinning and then etched away SiO₂ with alkaline solution to obtain porous structures. MA materials with large and graded pore structures could be prepared by this

method. Chen et al. [41] obtained mesoporous carbon fiber (MCF) by electrostatic spinning and subsequent HF etching. The pore structure of MCF could be adjusted by controlling the amount of tetraethyl orthosilicate. When the amount of tetraethyl orthosilicate was 0.50 mL, the pore structure of the prepared MCF was the most suitable for MA. When the thickness of MCF was 2.6 mm, the minimum reflection loss (RL_{min}) was −61.2 dB and the maximum effective absorption bandwidth (EAB) was 4.9 GHz.

High-temperature degradation materials were added to the raw materials for electrospinning, and the porous structure was formed by subsequent heat treatment. Abdalla et al. [42] successfully prepared 1D MA materials with microporous distribution by using PVP as a pore-forming agent. Using the thermal decomposition properties of PMMA, Zuo et al. [43] prepared porous magnetic carbon nanofibers (P-CNF/Fe) to effectively absorb low-frequency microwave, and explored the effect of porous nanostructures on MA. BET results showed that the pore size ranges from 30 to 100 nm. When the thickness of the materials was 4.1 mm, the RL_{min} was −44.86 dB and the maximum EAB was 3.28 GHz in the range of 12.96–16.24 GHz. Soft template method did not need complex equipment and had the advantages of simple method, convenient operation, low cost and so on, so it had been widely concerned. Using vegetable oil as a pore-forming agent, different evaporation rates of vegetable oil and DMF were used to form pore structure. Li et al. [44] prepared Ni/C porous nanofibers by using this method, and BET results showed that the pore sizes were mainly mesopores and micropores.

MOF materials had the advantages of low density, high porosity and large specific surface area, and its

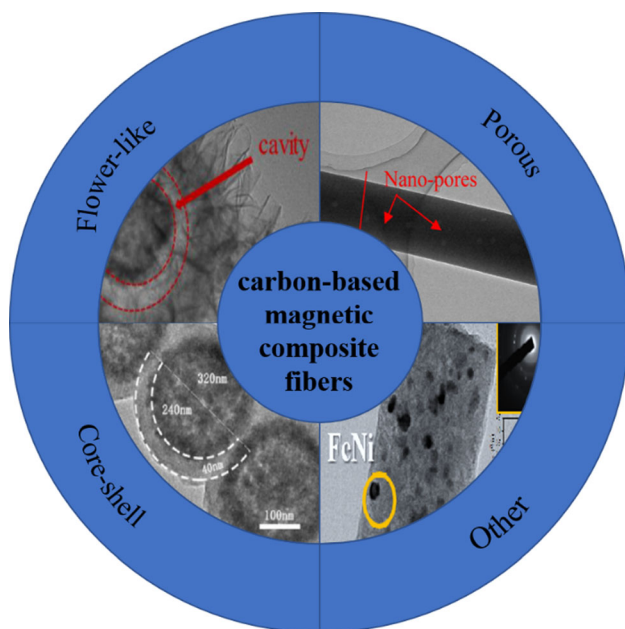


Figure 2 Various structures of carbon-based magnetic composite fibers. Reproduced with permission from Ref. [31–34].

porous structure could be retained after carbonization [45]. Therefore, MOF materials were often used to prepare porous materials. Chen et al. [46] successfully prepared 1D porous Fe^{III}-MOF-5-derived/carbon fibers composites (FMCFs) by using the method of electrospinning, and the synthesis process of FMCFs is shown in Fig. 3a. As can be seen in Fig. 3b, c, the Fe^{III}-MOF-5 in the fiber still retained the polyhedral structure. BET results showed that the specific surface area and pore volume of FMCF increased with the addition of Fe^{III}-MOF-5 (Fig. 3f, g). MOF material was an important method to prepare porous MA materials. Using CoZn-MOF as the precursor, Liao et al. [47] prepared porous Co/ZnO/C (CZC) microrods by pyrolysis with N₂. Figure 3d, e shows that CZC microrods had a high porosity structure. In addition, BET results showed that the surface area increases sharply with the increase in pyrolysis temperature (Fig. 3h, i), which was attributed to the release of 2-methylimidazole and some small molecules. Using ZIF-67-coated carbon fibers as

precursors, Quan et al. [48] embedded Co₃O₄-modified nitrogen-doped carbon array (triangular nanoplates) on the surface of carbon fibers in the carbon paper (NC-Co₃O₄/CP). The carbon fiber had a porous structure with pore size of micropores. When the thickness was 1.5 mm, the RL_{min} of NC-Co₃O₄/CP could reach -34.34 dB. Therefore, the porosity of MA materials could be controlled by adjusting the MOF amount and pyrolysis temperature to achieve strong MA.

Flower-like composites

The flower-like structure was usually fabricated by the irregular growth of the nanosheets to enhance microwave attenuation, which had the following advantages: (1) 1D flower-like structure could form conductive network to provide more conductive paths for electron transport. (2) The specific surface area of the MA materials could be greatly increased by coating the flower-like structure on the surface of the 1D materials. (3) Rough surfaces formed by the

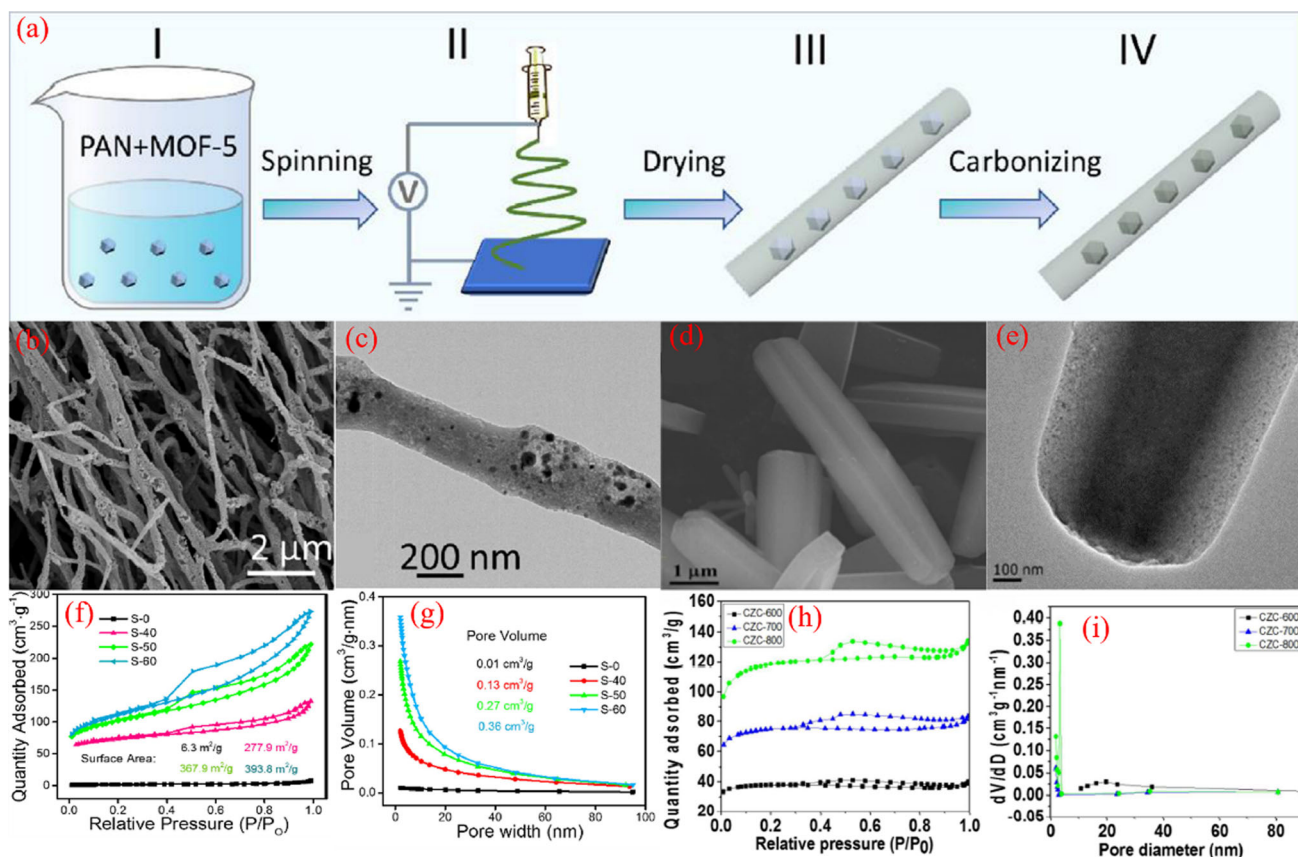


Figure 3 a, b BET information of FMCFs, c N₂ absorption isotherms and d pore size distributions of CZC-600, CZC-700 and CZC-800. Reproduced with permission from Ref. [46, 47].

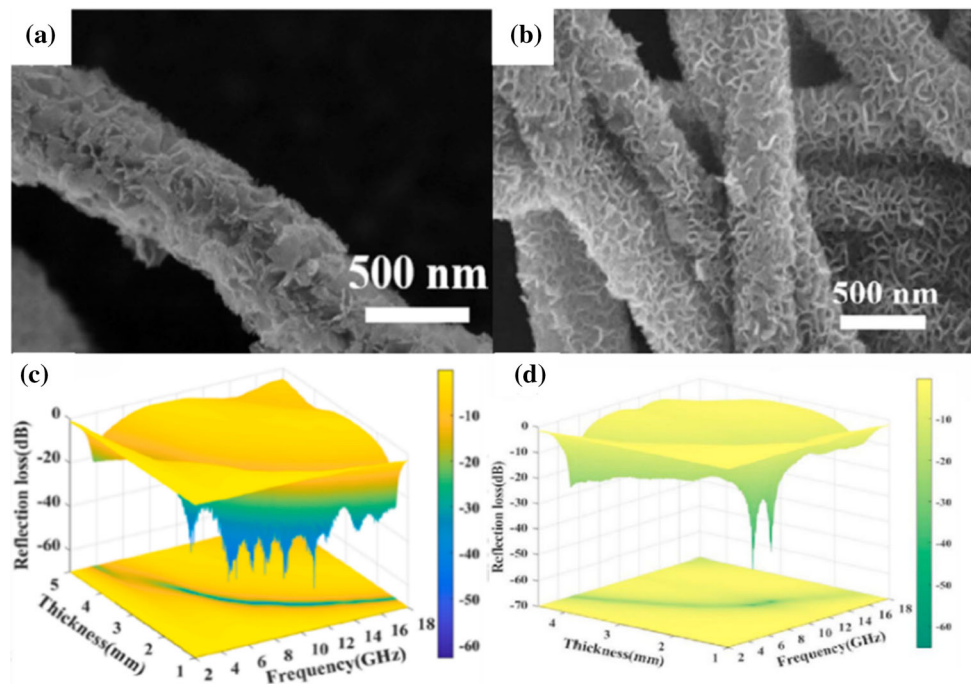
flower-like structure could induce multiple reflections and scatterings of microwave [49, 50].

The electromagnetic parameters of 1D flower composites could be adjusted by changing the composition and structure of nanoflowers. Tong et al. [51] synthesized Ni nanowire by magnetic field induction method and then prepared Ni@Co₃O₄/RGO by annealing and hydrothermal reaction. Flower-like structure was formed by a large number of Co(OH)₂ nanosheets. After annealing, Co₃O₄ nanosheets with flower-like structure were obtained, as illustrated in Fig. 4a. When the thickness was 1.6 mm, the maximum EAB was 4.62 GHz, as shown in Fig. 4c. In a different attempt, Tong et al. [52] grew flower-like MoS₂ on the surface of Fe₃O₄/Fe@C nanofibers, and the microscopic morphology is investigated in Fig. 4b. Fe₃O₄/Fe provided magnetic loss, and C provided dielectric loss. MoS₂ was a kind of semiconductor material with non-centrosymmetric structure, and its flower-like structure increased the microwave attenuation ability of microwave absorbers. When the thickness of the absorber was 2.24 mm, the RL_{min} of Fe₃O₄/Fe@C@MoS₂ nanofibers was -53.79 dB at 11.12 GHz, and the corresponding EAB reached 4.4 GHz, as illustrated in Fig. 4d.

The multicomponent MA material had a larger specific surface area than the single-component MA material, and its electromagnetic parameters were

easier to adjust. Ma et al. [53] prepared 1D flower-like ZnFe₂O₄@SiO₂@C@NiCo₂O₄ (ZSCNC) nanochains with core-shell structure to achieve broadband MA, as shown in Fig. 5a. Figure 5b, c reveals the unique aspect ratio and shape of the ZSCNC. At a loading of 30 wt% and a thickness of 2.39 mm, the RL_{min} was -54.29 dB at 11.14 GHz and the EAB was 5.66 GHz (11.94–17.60 GHz), as investigated in Fig. 5d. Huang et al. [54] prepared ZnFe₂O₄@SiO₂@C@NiO (ZSCN)/rGO composites by a multi-step synthesis method, and the flower-like structure was formed by NiO nanosheets. When the thickness of ZSCN/rGO was 2.45 mm, the RL_{min} was -66.38 dB at 9.58 GHz and the EAB was 3.44 GHz (8.12–11.56 GHz). The magnetic field induction method greatly simplified the difficulty of synthesizing magnetic nanochains, and the flower-like structures on the magnetic chains greatly increased the absorption area. The flower-like structure was caused by the irregular growth of NiO nanosheets. Magnetic field induction was a common method for preparing 1D magnetic nanochains. Liao et al. [55] field-induced distillation-precipitation polymerization and high-temperature carbonization. The materials had a RL_{min} of -52.5 dB at 13.2 GHz with a thickness of 2.23 mm, and the EAB was 4.98 GHz (10.10–15.08 GHz).

Figure 4 SEM images of **a** Ni@Co₃O₄ nanowires, **b** Hierarchical Fe₃O₄/Fe@C@MoS₂ core-shell nanofibers. 3D RL plots of **c** Ni@Co₃O₄/RGO composites, **d** Hierarchical Fe₃O₄/Fe@C@MoS₂ core-shell nanofibers. Reproduced with permission from Ref. [51, 52].



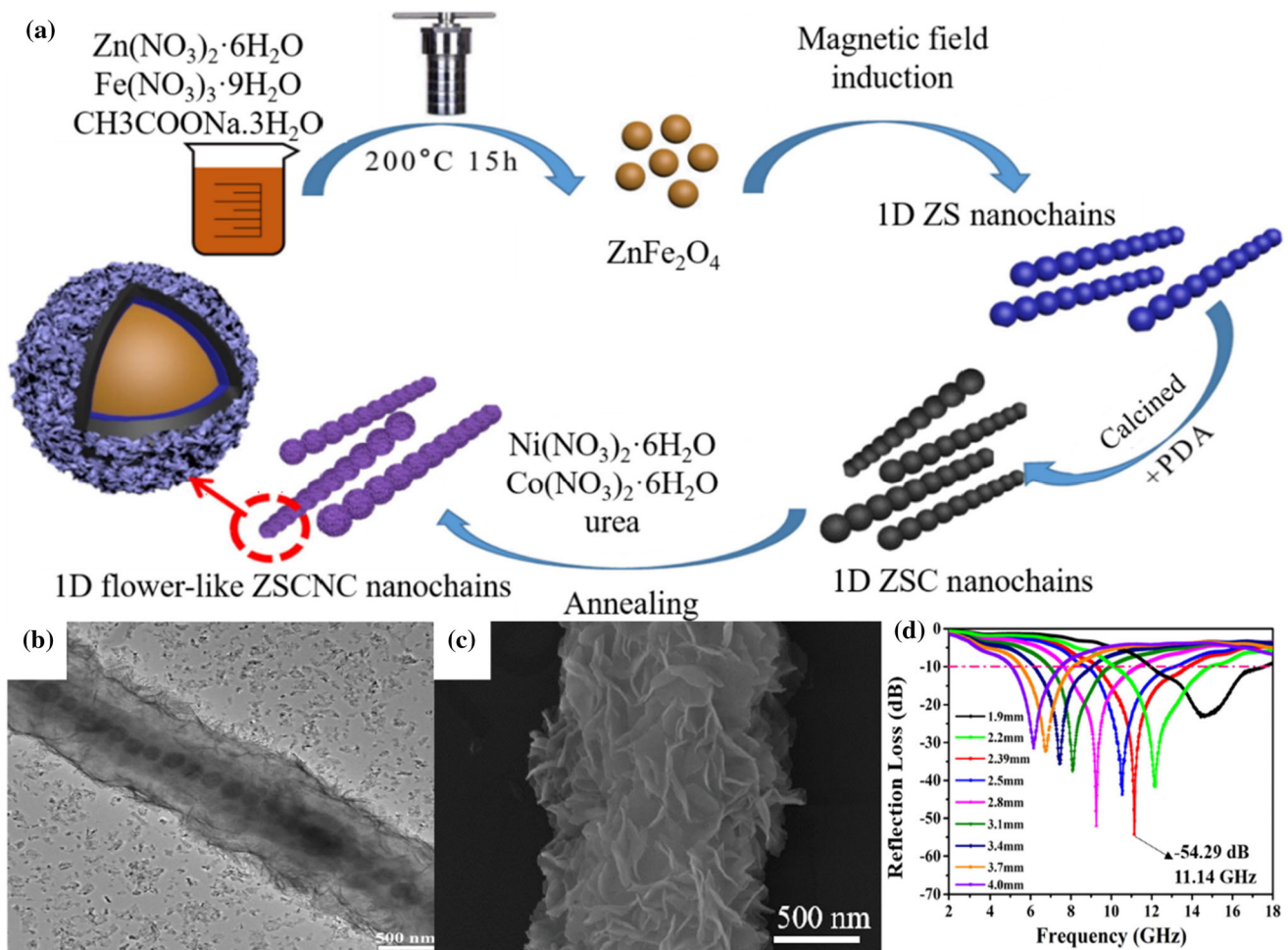


Figure 5 a Schematic illustration of the formation process of 1D flower-like ZSCNC nanochains, SEM images of **b** 1D flower-like ZSCNC nanochains, **c** TEM images of 1D flower-like ZSCNC

nanochains, **(d)** RL curves of the samples loaded with 1D flower-like ZSCNC nanochains. Reproduced with permission from Ref. [53].

Core–shell composites

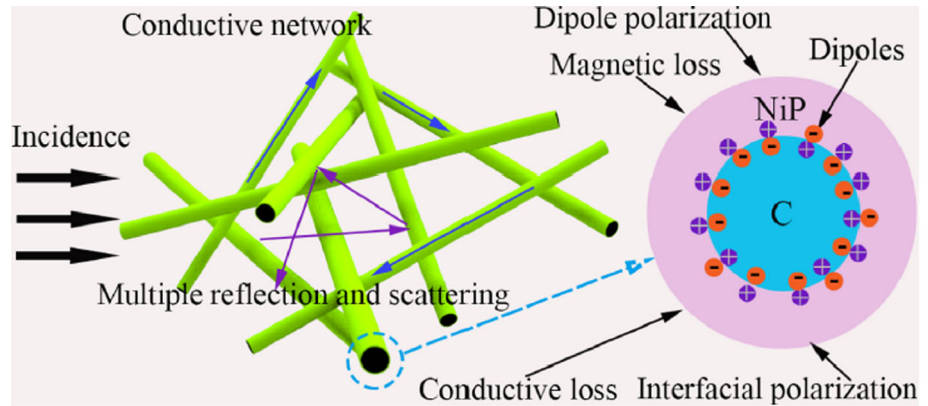
Core–shell structure was an assembly structure that orderly combined one material with another through chemical bonds or other forces. Recent studies had also shown that core–shell heterostructures played an important role in improving MA by means of space charge polarization and quantum confinement effect [56, 57]. In addition, core–shell nanocomposites also helped to combine the advantages of different materials to obtain new chemical and physical properties [58].

The common MA mechanism of carbon-based magnetic composites with 1D core–shell structure is investigated in Fig. 6. 1D core–shell microfiber composites attenuated microwave energy by forming a continuous conductive network, inducing current and triggering multiple reflections. Moreover, the

interface between the core and shell of the MA fiber materials became the polarization center to provide the interfacial polarization [59, 60].

Carbon fibers could be easily prepared by electrostatic spinning and carbonization technology. Therefore, the preparation of 1D core–shell materials based on electrostatic spinning technology had been widely reported. Liu et al. [61] prepared MA materials with carbon fibers and carbonyl iron composites by chemical vapor deposition. The carbonyl iron layer was uniformly adhered to the surface of carbon fiber as a shell. The RL_{\min} of the absorber was -21.5 dB at a thickness of 2 mm. The core–shell structure of carbonyl iron@carbon fiber was too single, so that the MA performance was not ideal. On this basis, magnetic nanoparticles could be used to modify the core–shell materials to obtain better MA properties. Qiao

Figure 6 Schematic illustration of the possible absorbing electromagnetic wave mechanism in C/NiP microfibers composites. Reproduced with permission from Ref [60].



et al. [62] prepared Ni-embedded TiO₂/C core-shell terpolymer nanofibers using a combination of electrospinning and heat treatment, with carbon fiber as the core and Ni-coated TiO₂ layer as the shell (Fig. 7a, b). The extremely large interface, conductive network and rough surface structure were the main sources of electromagnetic wave attenuation. Figure 7c shows that the RL_{min} of Ni-embedded TiO₂/C could reach -74.5 dB when the thickness was 2 mm.

The dielectric shell materials had good chemical corrosion resistance to protect the magnetic core materials, and the core-shell structure combining with the magnetic core and dielectric shell was often used to prepare MA materials. Cui et al. [63] successfully prepared FeCo/PVP core-shell nanochains@GO composites (FCPG) by reduction method. It could be clearly seen that PVP was uniformly coated on FeCo magnetic nanochains. This core-shell structure enhanced the interfacial polarization of FeCo nanocrystals and the stability of magnetic materials to acquire good MA properties. The RL_{min}

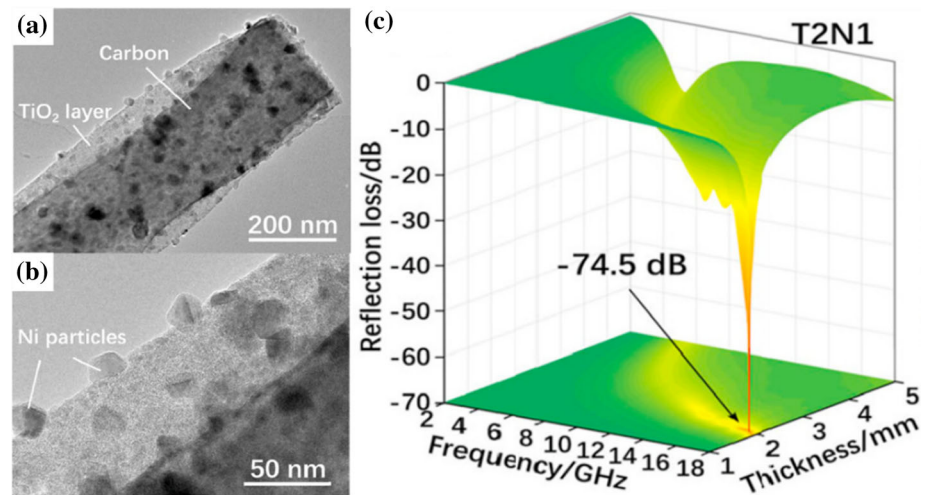
of FCPG was -52.5 dB at 13.2 GHz with a thickness of 2.23 mm, and the maximum EAB was 4.9 GHz.

In addition to the above structures, carbon nanofiber@core-shell nanoparticles were also important 1D core-shell materials. The multiple components and well-designed microstructures account for their excellent performance. Meng et al. [64] prepared C/Co nanofibers by simple electrostatic spinning and in situ reduction. Co nanospheres promoted the graphitization of carbon and formed core-shell Co/C on the surface of carbon fibers. Therefore, C/Co nanofibers had excellent corrosion resistance. When the thickness of C/Co nanofibers was 3.5 mm, the RL_{min} was -58.8 dB at 7.4 GHz, and the EAB was 12.9 GHz.

Other composites

Core@void@shell structure had the advantages of low density, large specific surface area and adjustable gaps, so core@void@shell was a highly

Figure 7 a, b HR-TEM images of T2N1, c 3D RL representation of T2N1. Reproduced with permission from Ref. [62].



efficient electromagnetic absorbing structure. Qiao et al. [65] prepared $\text{Fe}_3\text{O}_4@\text{void}@\text{SiO}_2$ and $\text{Fe}_3\text{O}_4@\text{void}@\text{SiO}_2@\text{PPy}$ (FVSP) MA materials with yolk-shell structure and compared their absorbing properties. Because PPy was a good dielectric loss material, FVSP nanochain had stronger MA performance than FVS nanochain.

Coating magnetic nanoparticles inside carbon nanotubes could greatly increase the corrosion resistance and interface area of materials. Xu et al. [66] successfully coated Fe/ Fe_3C nanospheres inside nitrogen-doped CNTs (Fe/ $\text{Fe}_3\text{C}@\text{NCNTs}$), resulting in a unique pea-like structure. The materials were prepared by heating $\text{FeCl}_3 \cdot 6\text{H}_2\text{O}$ and melamine in an inert atmosphere at a ratio of 1:1, and its chemical composition and microstructure were affected by pyrolysis temperature. Therefore, the electromagnetic parameters of the materials could be adjusted by controlling the pyrolysis temperature, and the rule was that the dielectric loss decreased with the increase in pyrolysis temperature. When the pyrolysis temperature was 600 °C and the thickness was 4.97 mm, the RL_{\min} was -46 dB at 3.6 GHz. Rough surfaces could increase the absorption properties of MA materials [67]. In Fig. 8a, Wang et al. [68] prepared magnetic Ni@C nanofibers with branched multi-walled CNTs (MWCNTs) by a two-step method of electrostatic spinning and in situ pyrolysis. In Fig. 8b, the branch of carbon nanofiber was MWCNTs grown under the catalysis of Ni crystal. This multi-branched 1D structure not only increased the surface area of MA materials, but also easily formed 3D conductive network. When the thickness was 1.5 mm, the RL_{\min} of Ni@C nanofibers was -53.2 dB and the EAB was 5.6 GHz (Fig. 8c).

The 1D MA materials with unique spiral shape could be crosslinked into networks to increase cross-linked polarization and conduction losses. Using Fe/Sn-nanoparticles as catalysts, Zuo et al. [69] prepared nanohelical coils by chemical vapor deposition. ZIF-67 was coated on their surface, and then Co@N-Carbon/CNCs was synthesized by pyrolysis of ZIF-67/CNCs at different temperatures. The results showed that the EAB of Co@N-Carbon/CNCs reached 5.5 GHz when the filling rate was only 6 wt%.

With the development of 1D carbon fibers, more and more 1D carbon fibers had been used to prepare MA materials. The RL_{\min} and the EAB of these similar materials are shown in Table 1.

Magnetic CNTs composites

CNTs were seamless tubular structures consisting of 2D graphite sheets coiled around a central axis, which could be single-walled or multi-walled [72]. Among them, single-wall CNTs had higher conductivity than multi-wall CNTs at the same content due to their smaller pipe diameter and larger aspect ratio [73, 74]. As a typical 1D nanomaterials, CNTs had the advantages of corrosion resistance, high electrical conductivity, great high-temperature strength, and low density [75]. Magnetic CNTs composites retained the advantages of CNTs to a certain extent and improved the impedance matching of CNTs. The electromagnetic parameters of magnetic CNTs composites could be easily adjusted by combining them with different magnetic materials [76]. Therefore, magnetic CNTs composites showed great application potential in MA.

CNTs/alloy composites

Only using CNTs as MA materials lacked magnetic loss capability, so CNTs needed to be combined with magnetic alloy materials to improve impedance matching [76]. Magnetic alloy materials could generate a large number of phase interfaces, and the magnetic loss capability of microwave absorbers could be tuned by adjusting the composition of the alloy [77, 78]. Some of the nanoalloys were distributed inside the CNTs, so the CNTs could reduce the agglomeration of nanoalloys very well. In addition, CNTs provided more electron transport pathways for 1D MA materials.

Nitrogen doping could promote interfacial and dipole polarization, and nitrogen-doped CNTs (N-CNT) composites had been widely reported in recent years [79, 80]. Zhou et al. [81] designed and prepared a novel porous iron-based nanocomposite containing Fe_3C , Fe_3N , Fe ($\text{Fe}_x\text{C}_y\text{N}_z$) and N-CNT. Some of the magnetic nanoparticles were encapsulated inside the CNTs to reduce the agglomeration of magnetic nanoparticles. The RL_{\min} of $\text{Fe}_x\text{C}_y\text{N}_z/\text{N-CNT-1000}$ obtained under the pyrolysis condition of 1000 °C was -25.1 dB at a thickness of 4 mm. When the thickness range was 2–5 mm, the EAB was 8.2 GHz. Magnetic metal particles were often filled into the interior of CNTs to form rich interfaces between metal particles and NCNTs. In order to explore the MA properties of different magnetic metal particles

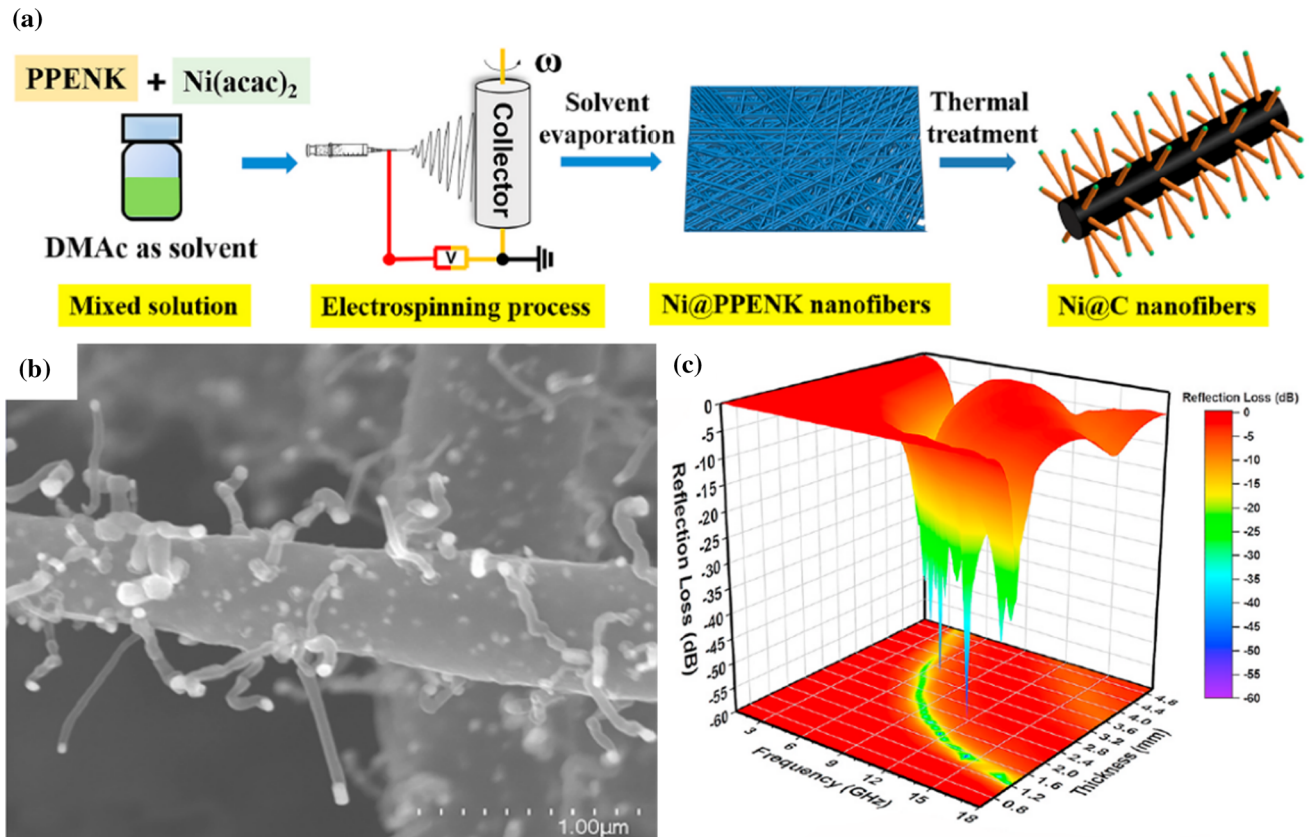


Figure 8 **a** Schematic diagram of the preparation process of Ni@C nanofibers, **b** SEM images of Ni@C nanofibers, **c** 3D-contour maps of RL values of Ni@C nanofibers. Reproduced with permission from Ref. [68].

combined with NCNTs, Ning et al. [82] successfully prepared the M@NCNTs composite materials (Fig. 9a–c), where M was Fe, Co, Ni nanoparticles. The curlier CNTs effectively avoided agglomeration of metal nanoparticles to obtain good MA performance. When the thickness was 3.2 mm, the RL_{\min} of Fe@NCNTs composite was -30.43 dB, and the EAB reached 5.7 GHz (Fig. 9g). Co@NCNTs and Ni@NCNTs also had satisfactory EAB of 4.08 GHz and 4.72 GHz, respectively. Similarly, Yang et al. [83] successfully prepared γ -FeNi/CNT nanocomposite particles by the wet chemical method, and γ -FeNi nanoparticles were uniformly distributed on the inside and outside of CNTs (Fig. 9d, e). When the sample thickness was 1.6 mm and the loading was 2 wt%, the RL_{\min} of γ -FeNi/CNTs at 16.5 GHz was -15.4 dB. Qi et al. [84] synthesized Fe/CNTs with core-shell structure by chemical vapor deposition, using hollow Fe_2O_3 particles as catalyst. The experiment used C_2H_2 to reduce Fe_2O_3 to Fe and then carbonized to form Fe_3C . Fe_3C could effectively catalyzed the growth of core-shell carbon

nano hybrid. As shown in Fig. 9f, Fe nanoparticles were uniformly encapsulated in CNTs. Due to the special structure of Fe/CNTs, the RL_{\min} was about -40.15 dB at the thickness of 1.5 mm, as shown in Fig. 9h. These excellent properties demonstrated that CNTs/alloy composites with 1D structures were efficient, sustainable MA materials.

Using CNTs as templates, MOF materials were grown on CNTs and further carbonized to prepare CNTs/alloy composites. Wang et al. [85] successfully designed CNTs fiber/Ni-MOF interpenetrating structure by solvothermal method to enhance carrier mobility. At a thickness of 5 mm, the RL_{\min} was -24.32 dB. CNTs had a large number of surface atoms and unsaturated suspended bonds, which were favorable for interfacial polarization and multiple scattering. Multi-walled CNTs (MWCNTs) were often used as fillers in MA materials because of their larger specific surface area. Yin et al. [86] used MWCNTs as raw materials to prepare Co-C/MWCNTs composites through pyrolysis precursor ZIF-67/MWCNTs. Under the induction of magnetic field, Co-C/

Table 1 The MA performance of magnetic carbon fiber composites

| Absorbers | Loading (wt%) | RL _{min} | | EAB | | References |
|--|---------------|-------------------|------------|----------------|-------------|------------|
| | | Thickness (mm) | Value (dB) | Thickness (mm) | Value (GHz) | |
| Co/PCNF | 17 | 5.21 | − 63.69 | 1.00–6.61 | 12.92 | [70] |
| Co/N–C nanofibers | 5 | 2.00 | − 25.70 | 2.00 | 4.30 | [39] |
| Fe ₃ C/N–C | 10 | 2.00 | − 29.10 | 2.00 | 4.10 | [40] |
| MCF | 30 | 2.60 | − 61.20 | 2.60 | 4.90 | [41] |
| C ₂ F ₂ T rGO ₂ @CNFs | – | 5.00 | − 43.60 | 1.00–5.50 | 13.70 | [42] |
| P-CNF/Fe | 20 | 4.10 | − 44.86 | 1.50 | 3.28 | [43] |
| Ni/C | 25 | 3.20 | − 69.50 | 2.50–5.50 | 12.80 | [44] |
| C-NiCo ₂ O ₄ | 50 | 1.90 | − 52.70 | 1.90 | 5.20 | [71] |
| FMCFs | 40 | 1.40 | − 39.20 | 1.40 | 4.40 | [46] |
| Porous CZC-700 | 30 | 3.00 | − 52.60 | 3.00 | 4.90 | [47] |
| NC-Co ₃ O ₄ /CP | 40 | 2.30 | − 41.38 | – | – | [48] |
| Fe ₃ O ₄ /Fe@C@MoS ₂ | 50 | 2.24 | − 53.79 | 2.24 | 4.40 | [52] |
| ZSCNC | 30 | 2.39 | − 54.29 | 2.39 | 5.66 | [53] |
| Ni@C ₃ O ₄ /RGO | 35 | 2.30 | − 60.00 | 1.60 | 4.62 | [51] |
| ZSCN/rGO | 50 | 2.45 | − 66.38 | 2.45 | 3.44 | [54] |
| ZnFe ₂ O ₄ /C/MoS ₂ /FeS ₂ | 50 | 2.23 | − 52.50 | 2.23 | 4.98 | [55] |
| Carbon fiber/carbonyl iron | 4 | 2.00 | − 21.50 | 0.90–3.90 | 2.00–18.00 | [61] |
| Ni-embedded TiO ₂ /C | 15 | 2.00 | − 74.50 | 2.60 | 6.70 | [62] |
| FCPG | – | 2.00 | − 40.94 | 2.00 | 4.90 | [63] |
| C/Co | 15 | 3.50 | − 58.80 | 3.50 | 12.90 | [64] |
| Fe ₃ O ₄ @N-doped carbon nanochains | 20 | 3.10 | − 63.09 | 3.10 | 5.34 | [65] |
| Branch-like Ni@C nanofibers | 20 | 1.50 | − 53.20 | 1.50 | 5.60 | [68] |
| Fe/Fe ₃ C@NCNTs | 30 | 4.97 | − 46.00 | 1.00–5.00 | 14.80 | [66] |
| Co@N-carbon/CNCs | 6 | 3.50 | − 47.00 | 2.20 | 5.50 | [69] |

MWCNTs had certain orientation in the paraffin matrix, and the effective dielectric constant was improved. When the filling rate of Co–C/MWCNTs was 15 wt%, the RL_{min} was − 48.9 dB.

Among the traditional preparation methods of CNTs, Fe [87], Co [88] and Ni [89] had been proved to be good metal catalysts for the preparation of CNTs. In addition, MOF materials (ZIF-8 [90], ZIF-67 [91], etc.) were easily reduced to metallic particles during carbonization, and these metallic particles acted as catalysts to convert MOF-derived carbon into CNTs. Therefore, researchers tended to use the method of in situ generation of CNTs to prepare MA materials. Wang et al. [92] prepared NiCo alloy/carbon nanorods decorated with CNTs by pyrolysis, and CNTs were grown in situ under the catalysis of NiCo nanoparticles. The rod-like structure and uniform mesoporous structure of NiCo-MOF-74 were well preserved in the NiCo alloy/carbon composites. Thus, by controlling the Ni/Co ratio in the precursor, the microstructure of the MA materials could be

easily tuned. In addition, CNTs on the fiber surface formed a conductive network to increase the attenuation capacity of materials. When MOFs were used as templates for the preparation of CNTs, dicyandiamide or melamine was often added as an additive [93]. Liu et al. [94] prepared Fe/Fe₃C@NCNTs by placing a ceramic vessel loaded with dicyandiamide in the air inlet during Fe-MOF pyrolysis. Bamboo-like NCNTs were coated on Fe/Fe₃C nanospheres. Fe/Fe₃C@NCNTs had a large number of defects, voids and interfaces, which greatly improved the polarization loss. When the thickness was 1.6 mm, the RL_{min} was − 50.8 dB. Xue et al. [95] successfully prepared Co/MnO/CNTs composites by pyrolysis of core-shell MnO₂/ZIF template. Under the catalysis of metal particles, CNTs grew in large quantities, and Co/MnO/CNTs composites showed caterpillar lamellar structure. The CNTs were intertwined with each other to form a complex mesh structure, which was favorable to generate multiple polarizations and resonances. When the thickness was 1.97 mm and the

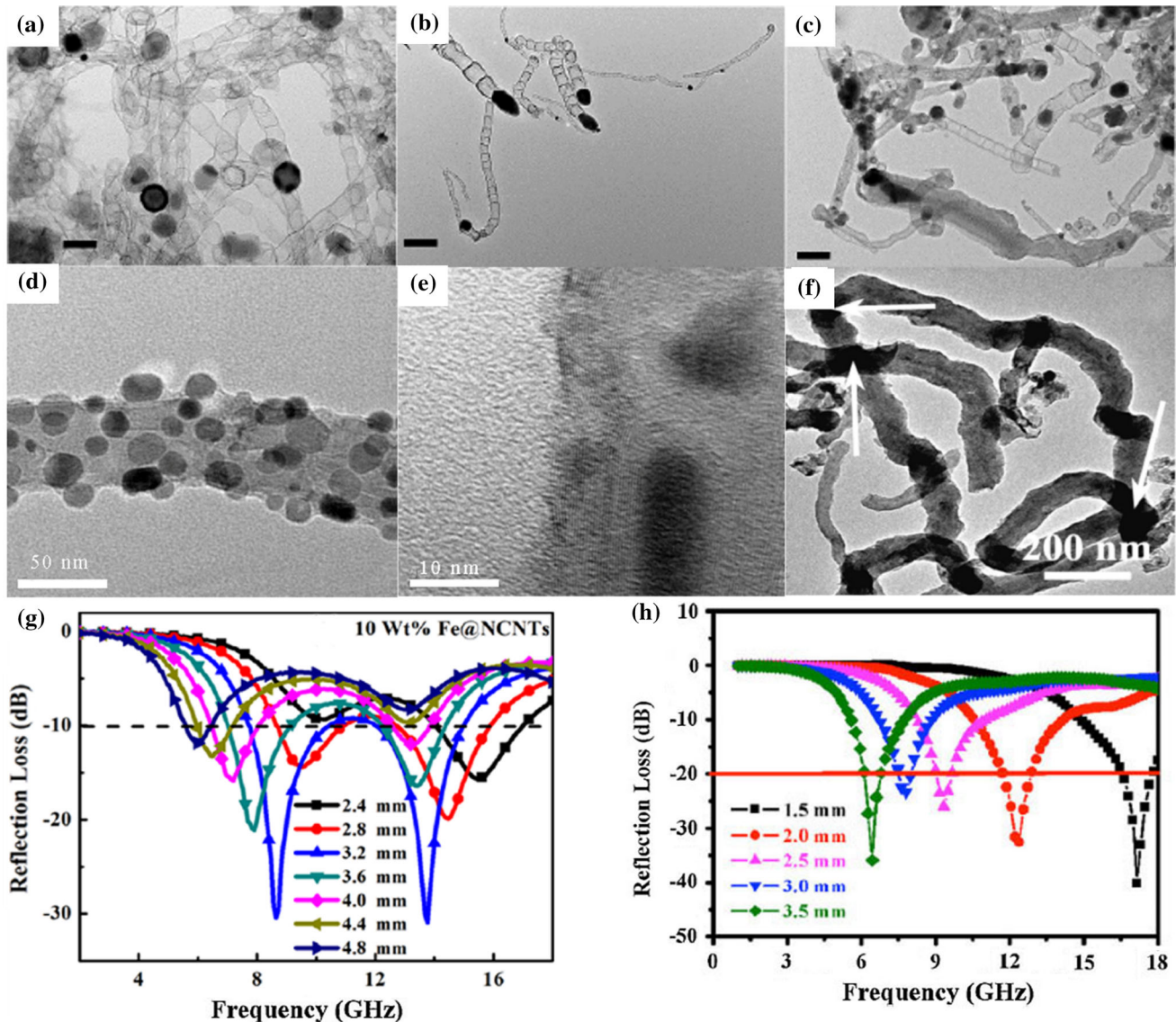


Figure 9 TEM images of **a** Fe@NCNTs, **b** Co@NCNTs and **c** Ni@NCNTs, **d** Local CNTs well coated with γ -FeNi alloys, **e** Local CNTs filled in with γ -FeNi alloys, **f** Fe/CNT hybrid. **g** RLs of Fe@NCNTs/wax with 10 wt% loadings under different

filling amount was 35 wt%, the RL_{min} was -58 dB and the EAB was 5.36 GHz. Without the use of templates, Wu et al. [96] self-assembled MXene and CoNi-bimetallic MOF into 1D heterostructural MA materials (MXene fibers@MOF-derived CNTs, MMC). By controlling the loading of MOFs on MXene fibers, the growth of CNTs could be effectively controlled, and the electromagnetic parameters could be regulated. The 1D structure of MMC was entangled to form a spatial network, which was beneficial to the conductivity of matrix. The thickness of MMC was only 1.6 mm, the RL_{min} was -51.6 dB, and the

thicknesses. **h** Absorption properties of Fe/CNTs composite with different thicknesses. Reproduced with permission from Ref [82–84].

maximum EAB was 4.6 GHz. In recent years, absorbers related to CNTs/allyo composites are shown in Table 2.

CNTs/ferrite composites

Ferrite was widely used as MA materials with high permeability, high resistivity and good impedance matching performance [97, 98], mainly through self-polarization, hysteresis loss, domain wall resonance and natural resonance to lose electromagnetic wave. Impedance matching of microwave absorbers could

be improved by compositing ferrite and CNTs[99]. Therefore, the combination of CNTs and ferrite was an effective method to improve MA performance.

Spinel ferrite, as a common crystal type, had high magneto-crystal anisotropy and saturation magnetization. Therefore, it was widely used in MA field [100–103]. Its molecular formula was MeFe_2O_4 , and Me was metal ion [104]. Fang et al. [105] mass-produced NiCo-SWCNTs in helium by DC arc discharge and prepared spinel CoFe_2O_4 nanocrystals by sol-gel spontaneous combustion. Then NiCo-SWCNTs/ CoFe_2O_4 nanocomposites were synthesized by mechanical mixing. As illustrated in Fig. 10a, b, many nanoparticles were uniformly attached to the long filamentous carbon. When the thickness of NiCo-SWCNTs/ CoFe_2O_4 was 1.80 mm, the EAB was 7.10 GHz (Fig. 10e). In addition to straight CNTs, spiral CNTs were also synthesized by the researchers. Feng et al. [106] prepared CoFe_2O_4 (CFO) nanoparticles coated with coiled CNTs (CCNTs) to form CCNTs/CFO composites. As shown in Fig. 10c, d, CFO was grown on the surface of helical CNTs with a large number of interfaces that are favorable to dipole polarization and interfacial polarization. At a thickness of 3 mm, the EAB of CCNTs/CFO was 4.4 GHz, as shown in Fig. 10f.

The distribution of magnetic particles on the fiber surface also affected the MA performance. Li et al. [107] prepared nano- Fe_3O_4 compact-coated CNTs (FCCs) and Fe_3O_4 loose-coated CNTs (FLCs) by the solvothermal method. Fe_3O_4 nanoparticles were evenly distributed on the surface of the two types of MA materials. In addition, CNTs and Fe^{3+} had the appropriate mass ratio in FCCs and FLCs to achieve

both strong dielectric and magnetic losses. The MA performance of FCCs was superior to that of FLCs, and the RL_{\min} of FCC was -43 dB at a thickness of 1.5 mm. Fe_3O_4 was a traditional magnetic loss material with high saturation magnetization, so it had been widely used in MA field [108]. Ren et al. [109] synthesized CNTs loaded with Fe_3O_4 by chemical vapor deposition method. The MA capacity of a single iron oxide on CNTs was limited. When the thickness of the composites was 3 mm, the RL_{\min} was -35.9 dB at 7.12 GHz. When the thickness was 1.5 mm, the EAB was 4.32 GHz. Similarly, Fe_3O_4 nanoparticles were used to enhance the magnetic loss capacity of microwave absorber. Alanagh et al. [110] prepared $\text{Fe}_3\text{O}_4/\text{MWCNTs@CFs}$ nanocomposites by introducing MWCNTs and Fe_3O_4 nanoparticles into carbon fibers through electrophoretic co-deposition process. $\text{Fe}_3\text{O}_4/\text{MWCNTs@CFs}$ nanocomposites had a large number of mesoporous structures. Compared with the two-component MA materials, the three-component $\text{Fe}_3\text{O}_4/\text{MWCNTs@CFs}$ had more interfaces, producing more interfacial polarization. The EAB was about 8 GHz at a thickness of 2 mm and a filling amount of 20 wt%. Direct contacts between MWCNTs and Fe layers were prevented by amorphous carbon layers to inhibit inverse radiation and eddy currents. Wu et al. [111] first prepared MWCNTs@C by in situ polymerization and high-temperature carbonization and then obtained the MWCNTs@C@ Fe_xO_y ($\text{Fe}/\alpha\text{-Fe}_2\text{O}_3$) composite by subsequent heat treatment. MWCNTs interweaved into conductive networks both to increase the electron conduction pathway and to form a large number of interfaces with magnetic nanoparticles. The

Table 2 The MA performance of CNTs/ally composites

| Absorbers | Loading (wt%) | RL_{\min} | | EAB | | References |
|--|---------------|--------------------|------------|----------------|-------------|------------|
| | | Thickness (mm) | Value (dB) | Thickness (mm) | Value (GHz) | |
| $\text{Fe}_x\text{C}_y\text{N}_z/\text{N-doped CNT}$ | 12 | 4.00 | -25.10 | 2.00–5.00 | 8.20 | [84] |
| M@NCNTs | 10 | 3.20 | -30.43 | 3.20 | 5.70 | [85] |
| $\gamma\text{-FeNi/CNT/EP}$ | 2 | 1.60 | -15.40 | 1.60 | 3.80 | [86] |
| Fe/CNT | 30 | 1.50 | -40.15 | 1.50–8.00 | 0.50–18 | [87] |
| CNT/Ni-MOF | 25 | 5.00 | -24.32 | 1.00–5.00 | 4.00–18 | [88] |
| Co-C/MWCNTs | 15 | 2.99 | -48.90 | – | – | [89] |
| $\text{NiCo alloy/carbon nanorod@CNT}$ | 5 | 2.20 | -43.70 | 2.20 | 2.50 | [95] |
| $\text{Fe/Fe}_3\text{C@NCNTs}$ | 40 | 1.60 | -50.8 | 1.40 | 4.30 | [97] |
| Co/MnO/CNTs | 35 | 2.65 | -58.00 | 1.97 | 5.36 | [98] |
| MMC | 50 | 1.60 | -51.60 | 1.50 | 4.60 | [99] |

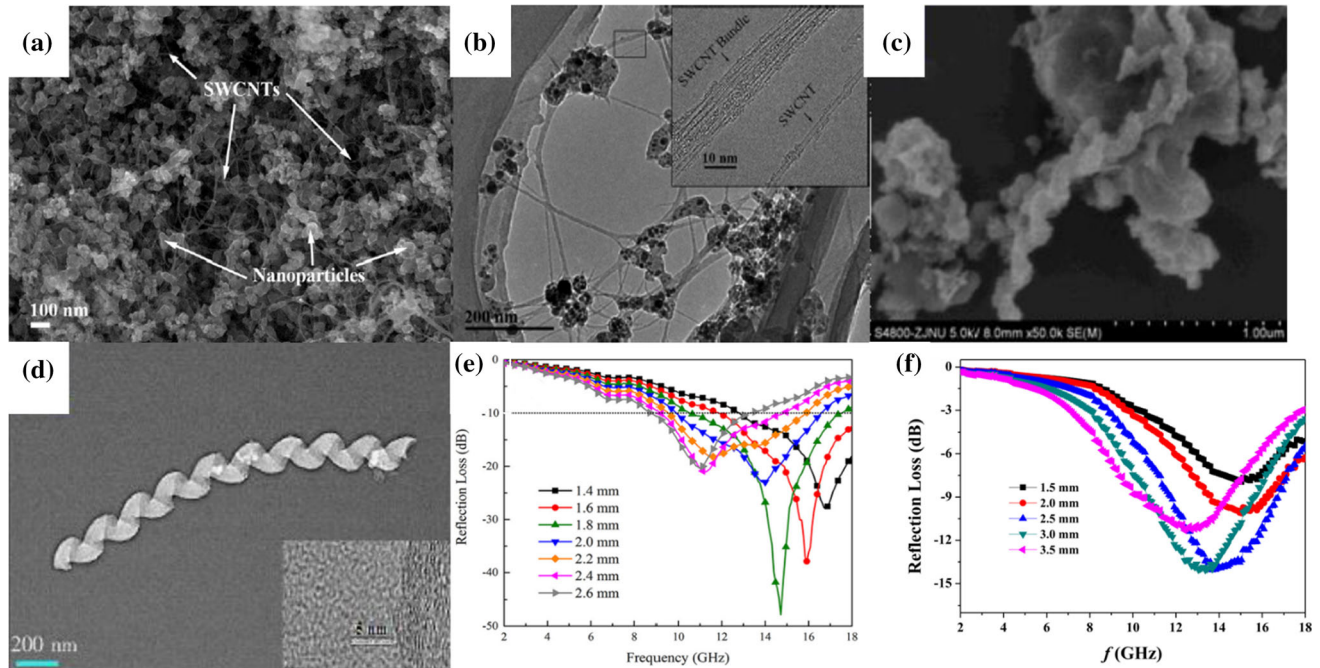


Figure 10 A typical **a** SEM image and **b** TEM image of the as-grown NiCo-SWCNTs. The inset in **(b)** is a HR-TEM image taken from the square region marked in **(b)**. **c** SEM image of CCNTs composite with $\omega_{\text{CCNT}}/\omega_{\text{CFO}}$ of 0.6. **d** TEM image of CCNTs.

materials had an EAB of 4.6 GHz at a thickness of 1 mm. More examples of CNTs/ferrite composites are summarized in Table 3.

Magnetic biomass-derived carbon composites

Biomass resources were natural carbon-based carriers, which had the characteristics of various types, wide sources, good porosity, and rich carbon content [115, 116]. The preparation of carbon-based MA materials from biomass had become a new sustainable and low-cost method [117]. Natural biomass usually had fine microtubule channels and heterostructures, which was difficult to achieve by conventional chemical synthesis. Using natural and unique microstructure characteristics to optimize the MA performance was an effective way to deal with the growing electromagnetic interference problem. Cotton was often used as a precursor of carbon fiber in the field of MA due to its wide availability and low cost. Li et al. [118] successfully prepared Co/C fiber by impregnation and calcination using cotton as carbon source. The MA properties of Co/C fibers

e The RL for the NiCo-SWCNTs nanocomposites at different thicknesses. **f** The RL of CCNTs/CFO composite with $\omega_{\text{CCNT}}/\omega_{\text{CFO}}$ of 0.6. Reproduced with permission from Ref. [105, 106].

with different Co contents were investigated. The maximum EAB of Co/C fibers reached 6.7 GHz at a thickness of 2.5 mm. Using cotton as the precursor of carbon fiber, Yin et al. [119] prepared CFs@H-Fe₃O₄/CoFe hybrids using a simple two-stage method of hydrothermal and calcination. The Fe₃O₄ nanospheres on the surface of carbon fiber had hollow structure. CFs@H-Fe₃O₄/CoFe had good low-frequency absorption capacity. The RL_{min} of CFs@H-Fe₃O₄/CoFe was -40.85 dB with a thickness of 3.5 mm.

However, biomass-derived 1D carbon-based magnetic composites prepared by impregnation and pyrolysis of metal ions often produce agglomeration. To explore more complex structures, the researches tried to combine the MOFs with carbon fibers. Using cotton and MOF as raw materials, Yang et al. [120] prepared hierarchical carbon fiber coated with Co/C dodecahedron nanoparticles and villus-like CNTs (HCF@CZ-CNTs). The apparent density of the material was as low as 0.0198 g/cm³. When the thickness was 2.0 mm, HCF@CZ-CNTs exhibited the RL_{min} value of -53.5 dB at 7.8 GHz and the EAB of 8.02 GHz. Li et al. [121] prepared Fe-MOFs/biomass-cotton-derived Fe@nano-porous carbon@carbon fiber

Table 3 The MA performance of CNTs/ferrite composites

| Absorbers | Loading (wt%) | RL _{min} | | EAB | | References |
|---|---------------|-------------------|------------|----------------|-------------|------------|
| | | Thickness (mm) | Value (dB) | Thickness (mm) | Value (GHz) | |
| NiCo-SWCNTs/CoFe ₂ O ₄ | 15 | 1.80 | − 47.90 | 1.80 | 7.10 | [105] |
| CCNTs/CFO | 66 | 3.00 | − 14.40 | 3.00 | 4.40 | [106] |
| FCC | 30 | 1.50 | − 43.00 | 1.75 | 8.30 | [107] |
| CNTs loaded Fe ₃ O ₄ | – | 3.00 | − 35.90 | 1.50 | 4.32 | [109] |
| Fe ₃ O ₄ /MWCNTs@CFs | 20 | 2.00 | − 17.10 | 5.00 | 8.00 | [110] |
| MWCNTs@C@Fe _x O _y | 40 | 1.00 | − 12.20 | 1.00 | 4.60 | [111] |
| CNT/BaFe ₁₂ O ₁₉ | – | – | − 43.90 | 1.50 | 3.90 | [112] |
| Li-Zn ferrite/CNT | 86 | 5.00 | − 34.00 | 5.00 | 5.20 | [113] |
| CNT/graphite/BaFe ₁₂ O ₁₉ | 25 | 1.00 | − 45.80 | 1.00 | 4.20 | [114] |

(Fe@NPC@CF) composites by in situ synthesis and thermal decomposition. The results showed that the composites were well combined with the Fe@NPC composites uniformly dispersed on the carbon fiber. The composite material had a strong MA performance. When the matching thickness was 2.5 mm, the RL_{min} was − 46.2 dB, and the EAB was 5.2 GHz. In recent years, ZIF-67 had been used to prepare Co/C composites because of its high porosity, simple preparation and large pore size. Zhao et al. [122] prepared carbon-cotton/Co@NPC composites by pyrolysis cotton/ZIF-67, as shown in Fig. 11a. The carbon-cotton/Co@NPC retained the dodecahedron shape of ZIF-67 well (Fig. 11b, c), and its unique hierarchical and porous structure made the materials have good MA properties. When the thickness was 1.65 mm, the EAB was 4.4 GHz and the RL_{min} was − 51.2 dB (Fig. 11d).

A large amount of biomass waste was generated every year around the world, and these biomass waste could be used as raw materials to prepare various carbon-based composite materials, such as anode materials [123], biofuels [124], and microwave absorbers [125, 126]. At present, biomass waste as green and cheap carbon precursor had received extensive attention. Cellulose was a cheap and readily available natural material on the earth and was found in many agricultural residues (rice husks, wheat straw, bagasse, etc.). Using these agricultural residues as precursors of carbon materials, waste could be turned into treasure. Wei et al. [127] prepared Ni/C 1D MA materials by carbonization treatment with cellulose as raw materials. The RL_{min} of Ni/C composites at a thickness of 4.5 mm was −

53.8 dB (at 4.72 GHz). Biomass was used as a precursor for 1D carbon materials mainly due to the existence of natural structure (hollow structure [128], porous structure [129], layered fiber structure [130]). Zhang et al. [128] selected raw cattail tube with natural hollow structure as carbon precursor and synthesized MoS₂@Fe₃O₄@CT hybrid by hydrothermal method, carbonization, surface modification and electrostatic self-assembly. Fe₃O₄ nanoparticles were surrounded by MoS₂ nanosheets to form a flower-like core-shell structure. The RL_{min} of 1D MoS₂@Fe₃O₄/CT hybrids was − 62 dB at 2.09 mm, and its EAB was 6.8 GHz at 2.35 mm.

The porous structure of biomaterials promoted the entry of metal ions into the MA materials and provided a large number of active sites for the growth of magnetic materials [131]. Liu et al. [129] prepared lightweight porous Fe₃O₄/CF composites by in situ growth and graphitization using sugarcane bagasse as a low-cost carbon source. The Fe₃O₄/CF composites retained the natural porous structure of bagasse to obtain good MA capacity. Fan et al. [132] impregnated reed with Fe(NO₃)₃ and carbonized to prepare Fe@Fe₃C/C nanocomposites. Due to the capillary effect of the porous microstructure, Fe³⁺ was better impregnated into reed stalks. After calcination, the interfacial reaction between Fe and C formed Fe@Fe₃C with a core-shell structure. When the thickness was only 1.43 mm, the EAB was 4.57 GHz. In addition, the biological waste fibers produced by the plane tree polluted the living environment of human beings and also caused waste of biomass resources. Wu et al. [133] prepared ultra-light magnetic helical porous carbon fibers (MHPFs)

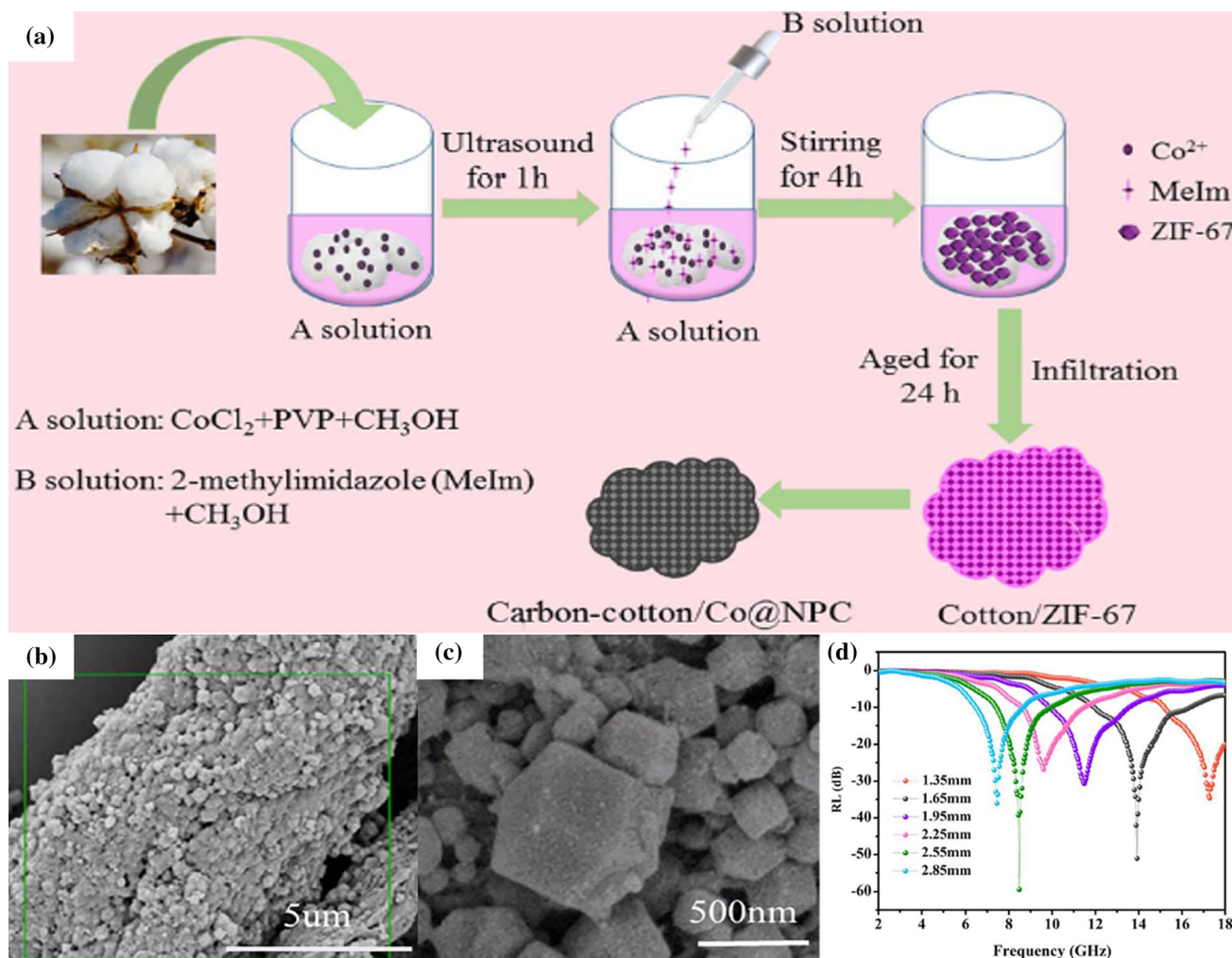


Figure 11 **a** Schematic illustration of the synthesis process of carbon-cotton/Co@NPC composites, **b** carbon-cotton/Co@NPC composites, **c** Amplified image of (b), **d** The RL values versus

different thickness of carbon-cotton/Co@NPC. Reproduced with permission from Ref. [122].

using biomass-inspired platanus (plane tree) fibers as the matrix (Fig. 12a). They developed a catalytic self-deposition (CSD) technique to achieve the confined growth of Ni nanoparticles in CNTs. Figure 12b, c reveals the carbon fibers were 1D hollow bamboo node-like morphology, and its surface was smooth with twisted texture. When the thickness of MHPFs-2.5 was 3.4 mm, the RL_{min} was - 55.39 dB.

In addition to plant fibers, natural collagen fibers extracted from animal bodies could also be used as precursors of carbon materials. Using natural collagen fiber as biological template, Wang et al. [130] successfully prepared ferromagnetic hierarchical carbon nanofiber bundles (FHCNBs). Furthermore, the EAB and absorption intensity of FHCNBs could be effectively adjusted by changing the ferromagnetic

materials (Fe₃O₄, Fe₃N, α-Fe, FeTiO₃/Fe₃O₄ and ZrO₂/Fe₃O₄) embedded on FHCNBs. This hierarchical nanofibrous structure of FHCNBs not only provided a smooth channel for microwave penetration, but also induced multiple reflections and scattering, thus obtaining excellent MA performance. Considering the superior properties of MOF materials, Zhao et al. [134] coated CoNi-bimetallic MOFs on bamboo carbon fiber and then obtained magnetic porous bamboo fiber/CoNi alloy (CN-ABF) by carbonizing. The unique porous structure of organisms greatly increased the specific surface area of carbon materials to increase the microwave attenuation of materials. Fang et al. [135] successfully synthesized carbon microtube and Co particle composite (CMT/Co) through Co salt impregnation and carbonization

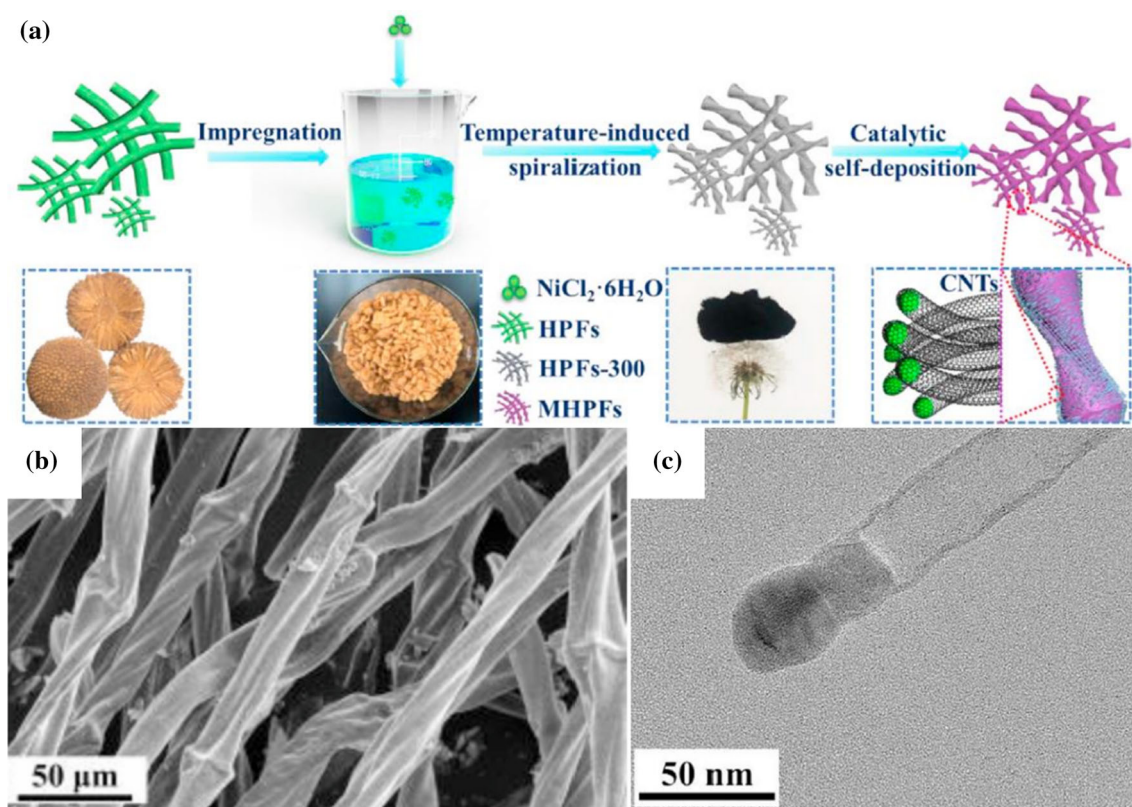


Figure 12 a Synthesis diagram of MHPFs. SEM images of b MHPFs-5, c HR-TEM of CNTs deposited on MHPFs-2.5. Reproduced with permission from Ref. [133].

process. Porous carbon microtube/Co particle composite (PCMT/Co) were synthesized by treating carbon fibers with H_3PO_4 and Co salt. PCMT/Co and CMT/Co still maintained the hollow microstructure of cotton fiber after the carbonization process. Co nanoparticles were uniformly distributed on the cotton-derived hollow carbon tubes. The surface of PCMT/Co was rougher and more porous than CMT/Co due to the addition of phosphoric acid. When the thickness was 1.4 mm, the RL_{min} of PCMT/Co was -36.8 dB. The RL_{min} of CMT/Co was -31.2 dB. Magnetic biomass-derived carbon composites showed great potential in MA, as listed in Table 4.

Conclusions and perspectives

Recent development of 1D carbon-based magnetic composites as a promising absorption candidate was proposed in this work. The outstanding advantages of different 1D materials are summarized systematically, which provides a basis for the future study of 1D magnetic carbon-based microwave absorption

materials. Common 1D carbon included carbon fiber, CNTs, and biomass-derived carbon, which had unique advantages in combination with magnetic materials. In the case of carbon fiber, the 1D porous structure reduced the density of MA materials and increased the times of microwave reflection. The irregular growth of the nanosheet formed a 1D flower-like structure, which greatly increased the specific surface area and the roughness of the absorbing materials. Core-shell heterostructure could generate space charge polarization to increase the polarization loss of MA materials. The preparation method of magnetic CNTs composites was flexible, and cross-linked CNTs provided abundant loss pathways for MA. The carbon fiber derived from biomass could retain the structure of biological materials itself, so it was suitable for preparing some structures that were difficult to be synthesized artificially. Different 1D structures had their own unique advantages for attenuating microwave energy. Therefore, a reasonable 1D structure was an important guarantee of MA performance.

Table 4 The MA performance of magnetic biomass-derived carbon composites

| Absorbers | Loading (wt%) | RL _{min} | | EAB | | References |
|--|---------------|-------------------|------------|----------------|-------------|------------|
| | | Thickness (mm) | Value (dB) | Thickness (mm) | Value (GHz) | |
| Co/C fiber | 33 | 2.00 | − 31.00 | 2.50 | 6.70 | [118] |
| CFs@H-Fe ₃ O ₄ /CoFe | 40 | 3.50 | − 40.85 | 1.50 | 2.14 | [119] |
| HCF@CZ-CNTs | 10 | 2.90 | − 53.50 | 2.00 | 8.02 | [120] |
| Fe@NPC@CF | 25 | 2.50 | − 46.20 | 2.50 | 5.20 | [121] |
| Carbon-cotton/Co@NPC | 25 | 2.55 | − 60.00 | 1.65 | 4.40 | [122] |
| MoS ₂ @Fe ₃ O ₄ /CT | 8 | 2.09 | − 62.00 | 2.35 | 6.80 | [128] |
| Fe ₃ O ₄ /CF | 30 | 1.90 | − 48.20 | 1.90 | 5.10 | [129] |
| Fe ₃ O ₄ -HCNBs | 80 | 2.00 | − 36.00 | 2.00 | 5.40 | [130] |
| Fe@Fe ₃ C/C | 30 | 2.05 | − 56.90 | 1.36 | 4.47 | [132] |
| MHPFs with CNTs | 5 | 3.40 | − 55.39 | 2.00 | 4.70 | [133] |
| CN-ABF | 80 | 2.66 | − 75.19 | 2.66 | 4.56 | [134] |
| PCMT/Co | 15 | 1.40 | − 36.80 | 1.40 | 6.70 | [135] |
| CMT/Co | 15 | 1.40 | − 31.20 | 1.40 | 5.50 | |

Although significant progress had been achieved in 1D carbon-based magnetic composites, they still faced many challenges. Firstly, current MA materials tended to composite various materials. However, due to the lack of detailed research on the significance of these materials combinations, there were blind spots in the preparation of multicomponent composite MA materials. The preparation of multicomponent MA materials was complicated and involved some toxic or polluting reagents. Secondly, the EAB of MA materials was usually concentrated in the high frequency region, while the study of low-frequency MA materials was not enough. Thirdly, most 1D carbon-based magnetic composites could not be used in harsh environments such as strong acid, high humidity and high temperature.

In order to solve the above problems, it was necessary to make full use of 1D carbon-based magnetic composites. The satisfactory microwave absorbers could be prepared by optimizing hybridization and constructing network structures. Furthermore, we believed that 1D carbon-based magnetic composites as outstanding absorbers would show greater potentiality. This review could provide guidance for the design of better 1D carbon-based magnetic composites in the future.

Acknowledgements

This work is financially supported by Natural Science Foundation of Shandong Province (No. ZR2021ME019, ZR2019BB063).

References

- [1] Shang T, Lu QS, Chao LM, Qin YL, Yun YH, Yun GH (2018) Effects of ordered mesoporous structure and L-doping on the microwave absorbing properties of CoFe₂O₄. *Appl Surf Sci* 434:234–242
- [2] Pawar SP, Bose S (2015) Extraordinary synergy in attenuating microwave radiation with cobalt-decorated graphene oxide and carbon nanotubes in polycarbonate/poly(styrene-co-acrylonitrile) blends. *Chemnanomat* 1:603–614
- [3] Wu NN, Liu C, Xu DM, Liu JR, Liu W, Liu H, Zhang JX, Xie W, Guo ZH (2019) Ultrathin high-performance electromagnetic wave absorbers with facilely fabricated hierarchical porous Co/C crabapples. *J Mater Chem C* 7:1659–1669
- [4] Wang F, Sun Y, Li D, Zhong B, Wu Z, Zuo S, Yan D, Zhuo R, Feng J, Yan P (2018) Microwave absorption properties of 3D cross-linked Fe/C porous nanofibers prepared by electrospinning. *Carbon* 134:264–273
- [5] Li ZX, Ding XL, Li F, Liu XG, Zhang SH, Long HM (2017) Enhanced dielectric loss induced by the doping of SiC in thick defective graphitic shells of Ni@C nanocapsules with ash-free coal as carbon source for broadband microwave absorption. *J Phys D: Appl Phys* 50:445305

- [6] Jiang Y, Chen Y, Liu YJ, Sui GX (2018) Lightweight spongy bone-like graphene@SiC aerogel composites for high-performance microwave absorption. *Chem Eng J* 337:522–531
- [7] Li M, Han M, Zhou J, Deng Q, Zhou X, Xue J, Du S, Yin X, Huang Q (2018) Novel scale-like structures of graphite/TiC/Ti₃C₂ hybrids for electromagnetic absorption. *Adv Electron Mater* 4:1700617
- [8] Zhang M, Ling HL, Ding SQ, Xie YX, Cheng TT, Zhao LB, Wang T, Bian HG, Lin H, Li ZJ, Meng AL (2021) Synthesis of CF@PANI hybrid nanocomposites decorated with Fe₃O₄ nanoparticles towards excellent lightweight microwave absorber. *Carbon* 174:248–259
- [9] Wei Y, Luo W, Li X, Lin Z, Hou C, Ma M, Ding J, Li T, Ma Y (2022) PANI-MnO₂ and Ti₃C₂T_x (MXene) as electrodes for high-performance flexible asymmetric supercapacitors. *Electrochim Acta* 406:139874
- [10] Luo W, Wei Y, Zhuang Z, Lin Z, Li X, Hou C, Li T, Ma Y (2022) Fabrication of Ti₃C₂T_x MXene/polyaniline composite films with adjustable thickness for high-performance flexible all-solid-state symmetric supercapacitors. *Electrochim Acta* 406:139871
- [11] Wei Y, Zheng M, Luo W, Dai B, Ren J, Ma M, Li T, Ma Y (2022) All pseudocapacitive MXene-MnO₂ flexible asymmetric supercapacitor. *J Energy Storage* 45:103715
- [12] Yang S, Xu DW, Chen P, Qiu HF, Guo X (2018) Synthesis of popcorn-like-Fe₂O₃/3D graphene sponge composites for excellent microwave absorption properties by a facile method. *J Mater Sci-Mater Electron* 29:19443–19453
- [13] Yin PF, Deng Y, Zhang LM, Wu WJ, Wang J, Feng X, Sun XY, Li HY, Tao Y (2018) One-step hydrothermal synthesis and enhanced microwave absorption properties of Ni_{0.5}Co_{0.5}Fe₂O₄/graphene composites in low frequency band. *Ceram Int* 44:20896–20905
- [14] Ma Y, Hou C, Zhang H, Zhang Q, Liu H, Wu S, Guo Z (2019) Three-dimensional core-shell Fe₃O₄/Polyaniline coaxial heterogeneous nanonets: preparation and high performance supercapacitor electrodes. *Electrochim Acta* 315:114–123
- [15] Zheng M, Wei Y, Ren J, Dai B, Luo W, Ma M, Li T, Ma Y (2021) 2-aminopyridine functionalized magnetic core-shell Fe₃O₄@polypyrrole composite for removal of Mn (VII) from aqueous solution by double-layer adsorption. *Sep Purif Technol* 277:119455
- [16] Bandaru S, Murthy N, Kulkarni R, English NJ (2021) Magnetic ferrite/carbonized cotton fiber composites for improving electromagnetic absorption properties at gigahertz frequencies. *J Mater Sci Technol* 86:127–138
- [17] Cheng Y, Seow JZY, Zhao HQ, Xu ZCJ, Ji GB (2020) A flexible and lightweight biomass-reinforced microwave absorber. *Nano-Micro Letters* 12:125
- [18] Zhao H, Cheng Y, Liu W, Yang LJ, Zhang BS, Wang LP, Ji GB, Xu ZCJ (2019) Biomass-derived porous carbon-based nanostructures for microwave absorption. *Nano-Micro Lett* 11(1):24
- [19] Wang C, Zong L, Li N, Pan Y, Liu Q, Zhang F, Qiao L, Wang J, Jian X (2021) Light-weight 1D heteroatoms-doped Fe₃C@C nanofibers for microwave absorption with a thinner matching thickness. *J Alloys Compd* 885:160968
- [20] Yin P, Zhang L, Tang Y, Liu J (2021) Earthworm-like (Co/CoO)@C composite derived from MOF for solving the problem of low-frequency microwave radiation. *J Alloys Compd* 881:160556
- [21] Li J, Zhang F, Lu H, Guo W, He X, Yuan Y (2021) Heterogeneous rod-like Ni@C composites toward strong and stable microwave absorption performance. *Carbon* 181:358–369
- [22] Guan G, Gao G, Xiang J, Yang J, Gong L, Chen X, Zhang Y, Zhang K, Meng X (2020) CoFe₂/BaTiO₃ hybrid nanofibers for microwave absorption. *ACS Appl Nano Mater* 3:8424–8437
- [23] Zhang YC, Shen YQ, Dang MM, Zhang F, Du XY (2021) In situ synthesis hydrophobic Co/CoO/C nanofibers with enhanced microwave absorption. *Ceram Int* 47:9178–9187
- [24] Yadav K, Kotabage C, Abhyankar AC (2021) NiCo₂O₄ nanoneedles decorated woven carbon fibres for electromagnetic shielding in X-band. *Mater Lett* 292:129622
- [25] Huang WB, Tong ZY, Wang RZ, Liao ZJ, Bi YX, Chen Y, Ma ML, Lyu P, Ma Y (2020) A review on electrospinning nanofibers in the field of microwave absorption. *Ceram Int* 46:26441–26453
- [26] Ma Y, Ma M, Yin X, Shao Q, Lu N, Feng Y, Lu Y, Wujcik EK, Mai X, Wang C, Guo Z (2018) Tuning polyaniline nanostructures via end group substitutions and their morphology dependent electrochemical performances. *Polymer* 156:128–135
- [27] Gill N, Sharma AL, Gupta V, Tomar M, Pandey OP, Singh DP (2019) Enhanced microwave absorption and suppressed reflection of polypyrrole-cobalt ferrite-graphene nanocomposite in X-band. *J Alloy Compd* 797:1190–1197
- [28] Ma Y, Zhuang Z, Ma M, Yang Y, Li W, Dong M, Wu S, Ding T, Guo Z (2019) Solid polyaniline dendrites consisting of high aspect ratio branches self-assembled using sodium lauryl sulfonate as soft templates: synthesis and electrochemical performance. *Polymer* 182:121808
- [29] Kaludjerovic BV, Sreckovic M, Janicijevic M, Kovacevic A, Bojanic S (2017) Influence of Nd³⁺: YAG laser

- irradiation on the properties of composites with carbon fibers. *Compos Pt B-Eng* 125:165–174
- [30] Zhao Z, Zhou X, Kou K, Wu HJC (2021) PVP assisted transformation of ZIF-67 into cobalt layered double hydroxide/carbon fiber as electromagnetic wave absorber. *Carbon* 173: 80–90
- [31] Lv J, Liang XH, Ji GB, Quan B, Liu W, Du YW (2018) Structural and carbonized design of 1D FeNi/C nanofibers with conductive network to optimize electromagnetic parameters and absorption abilities. *ACS Sustain Chem Eng* 6:7239–7249
- [32] Ma M, Li W, Tong Z, Yang Y, Ma Y, Cui Z, Wang R, Lyu P, Huang W (2020) 1D flower-like $\text{Fe}_3\text{O}_4@\text{SiO}_2@\text{MnO}_2$ nanochains inducing RGO self-assembly into aerogels for high-efficient microwave absorption. *Mater Des* 188:108462
- [33] Zhang T, Zhou PY, Xiao B, Zhang J, Wen GW, Zhong B, Xia L (2017) Controllable synthesis of porous C_xN_y nanofibers with enhanced electromagnetic wave absorption property. *Ceram Int* 43:8603–8610
- [34] Ma M, Li W, Tong Z, Huang W, Wang R, Lyu P, Ma Y, Wu G, Yan Q, Li P, Yao X (2020) Facile synthesis of the one-dimensional flower-like yolk-shell $\text{Fe}_3\text{O}_4@\text{SiO}_2@\text{NiO}$ nanochains composites for high-performance microwave absorption. *J Alloys Compd* 843:155199
- [35] Su H, Zhu P, Zhang L, Zhou F, Li G, Li T, Wang Q, Sun R, Wong C (2017) Waste to wealth: a sustainable and flexible supercapacitor based on office waste paper electrodes. *J Electroanal Chem* 786:28–34
- [36] Huo YS, Zhao K, Miao P, Li FP, Lu ZX, Meng QN, Tang YF (2021) Construction of tunable and high-efficiency microwave absorber enabled by growing flower-like TiO_2 on the surface of SiC/C nanofibers. *J Solid State Chem* 304:122553
- [37] Qiao J, Zhang X, Liu C, Zeng ZH, Yang YF, Wu LL, Wang FL, Wang Z, Liu W, Liu JR (2022) Facile synthesis of MnS nanoparticle embedded porous carbon nanocomposite fibers for broadband electromagnetic wave absorption. *Carbon* 191:525–534
- [38] Du H, Ai MQ, Lyu SS, Zhang PP, Chen XG, Jin AM, Ye Y (2022) Systematic fabrication and electromagnetic performance of porous biomass carbon/ferrite nanocomposites. *J Alloys Compd* 896:163048
- [39] Liu HH, Li YJ, Yuan MW, Sun GB, Li HF, Ma SL, Liao QL, Zhang Y (2018) In Situ preparation of cobalt nanoparticles decorated in n-doped carbon nanofibers as excellent electromagnetic wave absorbers. *ACS Appl Mater Interfaces* 10:22591–22601
- [40] Liu HH, Li YJ, Yuan MW, Sun GB, Liao QL, Zhang Y (2018) Solid and macroporous $\text{Fe}_3\text{C}/\text{N}-\text{C}$ nanofibers with enhanced electromagnetic wave absorptability. *Sci Rep* 8:16832
- [41] Chen JB, Liang XH, Zheng J, Gu WH, Pei CC, Fan FY, Ji GB (2021) Modulating dielectric loss of mesoporous carbon fibers with radar cross section reduction performance via computer simulation technology. *Inorg Chem Front* 8:758–765
- [42] Abdalla I, Elhassan A, Yu JY, Li ZL, Ding B (2020) A hybrid comprised of porous carbon nanofibers and rGO for efficient electromagnetic wave absorption. *Carbon* 157:703–713
- [43] Zuo XD, Xu P, Zhang CY, Li MZ, Jiang XY, Yue XG (2019) Porous magnetic carbon nanofibers (P-CNF/Fe) for low-frequency electromagnetic wave absorption synthesized by electrospinning. *Ceram Int* 45:4474–4481
- [44] Li DR, Guo K, Wang FY, Wu ZG, Zhong B, Zuo SY, Tang J, Feng JJ, Zhuo RF, Yan D, Yan PX (2019) Enhanced microwave absorption properties in C band of Ni/C porous nanofibers prepared by electrospinning. *J Alloys Compd* 800:294–304
- [45] Ma ML, Bi YX, Tong ZY, Liu YY, Lyu P, Wang RZ, Ma Y, Wu GL, Liao ZJ, Chen Y (2021) Recent progress of MOF-derived porous carbon materials for microwave absorption. *RSC Adv* 11:16572–16591
- [46] Chen JB, Zheng J, Wang F, Huang QQ, Ji GB (2021) Carbon fibers embedded with Fe^{III} -MOF-5-derived composites for enhanced microwave absorption. *Carbon* 174:509–517
- [47] Liao Q, He M, Zhou YM, Nie SX, Wang YJ, Hu S, Yang HY, Li HF, Tong Y (2018) Highly cuboid-shaped heterobimetallic metal-organic frameworks Derived from porous Co/ZnO/C microrods with improved electromagnetic wave absorption capabilities. *ACS Appl Mater Interfaces* 10:29136–29144
- [48] Quan B, Liang XH, Zhang X, Xu GY, Ji GB, Du YW (2018) Functionalized carbon nanofibers enabling stable and flexible absorbers with effective microwave response at low thickness. *ACS Appl Mater Interfaces* 10:41535–41543
- [49] Zhao ZH, Kou KC, Zhang LM, Wu HJ (2020) High efficiency electromagnetic wave absorber derived from transition metal layered double hydroxides. *J Colloid Interface Sci* 579:733–740
- [50] Luo J, Hu Y, Xiao L, Zhang G, Guo H, Hao G, Jiang W (2019) Synthesis of 3D flower-like Fe_3S_4 microspheres and quasi-sphere Fe_3S_4 -RGO hybrid-architectures with enhanced electromagnetic wave absorption. *Nanotechnology* 31:085708
- [51] Tong Z, Bi Y, Ma M, Liao Z, Huang W, Chung KL, Ma Y, Wu G, Qu Y, Pan C, Wang Y (2021) Fabrication of flower-

- like surface Ni@Co₃O₄ nanowires anchored on RGO nanosheets for high-performance microwave absorption. *Appl Surf Sci* 565:150483
- [52] Tong Z, Liao Z, Liu Y, Ma M, Bi Y, Huang W, Ma Y, Qiao M, Wu G (2021) Hierarchical Fe₃O₄/Fe@C@MoS₂ core-shell nanofibers for efficient microwave absorption. *Carbon* 179:646–654
- [53] Ma M, Li W, Tong Z, Ma Y, Bi Y, Liao Z, Zhou J, Wu G, Li M, Yue J, Song X, Zhang X (2020) NiCo₂O₄ nanosheets decorated on one-dimensional ZnFe₂O₄@SiO₂@C nanochains with high-performance microwave absorption. *J Colloid Interface Sci* 578:58–68
- [54] Huang W, Tong Z, Li W, Ma M, Bi Y, Liao Z, Wang R, Ma Y (2020) Fabrication of flower-like ZnFe₂O₄@SiO₂@C@NiO nanochains/reduced graphene oxides as a high-performance microwave absorber. *J Alloys Compd* 849:156658
- [55] Liao Z, Ma M, Tong Z, Bi Y, Chung KL, Qiao M, Ma Y, Ma A, Wu G, Li Z, Zhang Y (2021) Fabrication of one-dimensional ZnFe₂O₄@carbon@MoS₂/FeS₂ composites as electromagnetic wave absorber. *J Colloid Interface Sci* 600:90–98
- [56] Zhao B, Zhao WY, Shao G, Fan BB, Zhang R (2015) Morphology-control synthesis of a core-shell structured NiCu alloy with tunable electromagnetic-wave absorption capabilities. *ACS Appl Mater Interfaces* 7:12951–12960
- [57] Liu DW, Du YC, Xu P, Liu N, Wang YH, Zhao HH, Cui LR, Han XJ (2019) Waxberry-like hierarchical Ni@C microspheres with high-performance microwave absorption. *J Mater Chem C* 7:5037–5046
- [58] Huang YX, Zhang HY, Zeng GX, Li ZH, Zhang DF, Zhu HP, Xie RF, Zheng LM, Zhu JH (2016) The microwave absorption properties of carbon-encapsulated nickel nanoparticles/silicone resin flexible absorbing material. *J Alloys Compd* 682:138–143
- [59] Wei YP, Zhong KY, Jiang TT, Zhang JW, Bi KQ, Li LQ, Peng Y (2020) Gumdrop-cake-like CuNi/C nanofibers with tunable microstructure for microwave absorbing application. *Ceram Int* 46:11406–11415
- [60] Wei Y, Lin J, Jiang T, Li L, Zhong K, Zhang J, Peng Y (2021) Optimization of microwave absorption properties of C/NiP microfiber composites. *Ceram Int* 47:7937–7945
- [61] Liu Y, Liu XX, Li R, Wen W, Wang XJ (2015) Design and fabrication of carbon fiber/carbonyl iron core-shell structure composites as high-performance microwave absorbers. *RSC Adv* 5:8713–8720
- [62] Qiao J, Zhang X, Liu C, Lyu LF, Wang Z, Wu LL, Liu W, Wang FL, Liu JR (2020) Facile fabrication of Ni embedded TiO₂/C core-shell ternary nanofibers with multicomponent functional synergy for efficient electromagnetic wave absorption. *Compos Pt B-Eng* 200:108343
- [63] Cui ER, Pan F, Xiang Z, Liu ZC, Yu LZ, Xiong J, Li X, Lu W (2021) Engineering dielectric loss of FeCo/Polyvinylpyrrolidone core-shell nanochains@graphene oxide composites with excellent microwave absorbing properties. *Adv Eng Mater* 23:2000827
- [64] Meng XF, Dong SH (2019) Design and construction of lightweight C/Co heterojunction nanofibres for enhanced microwave absorption performance. *J Alloys Compd* 810:151806
- [65] Qiao MT, Lei XF, Ma Y, Tian LD, He XW, Su KH, Zhang QY (2018) Application of yolk-shell Fe₃O₄@N-doped carbon nanochains as highly effective microwave-absorption material. *Nano Res* 11:1500–1519
- [66] Xu Z, Du YC, Liu DW, Wang YH, Ma WJ, Wang Y, Xu P, Han XJ (2019) Pea-like Fe/Fe₃C nanoparticles embedded in nitrogen-doped carbon nanotubes with tunable dielectric/magnetic loss and efficient electromagnetic absorption. *ACS Appl Mater Interfaces* 11:4268–4277
- [67] Wang J, Li Q, Ren J, Zhang A, Zhang Q, Zhang B (2021) Synthesis of bowknot-like N-doped Co@C magnetic nanoparticles constituted by acicular structural units for excellent microwave absorption. *Carbon* 181:28–39
- [68] Wang C, Zong L, Pan Y, Li N, Liu Q, Wang J, Jian X (2021) Preparation and characterization of branch-like heteroatoms-doped Ni@C nanofibers for high-performance microwave absorption with thin thickness. *Compos Pt B-Eng* 223:109114
- [69] Zuo X, Zhao Y, Zhang H, Huang H, Zhou C, Cong T, Muhammad J, Yang X, Zhang Y, Fan Z, Pan L (2022) Surface modification of helical carbon nanocoil (CNC) with N-doped and Co-anchored carbon layer for efficient microwave absorption. *J Colloid Interface Sci* 608:1894–1906
- [70] Zhu YX, Wang SF, Zhang YS, Wu ZG, Zhong B, Li DR, Wang FY, Feng JJ, Tang J, Zhuo RF, Yan PX (2021) Large-scale preparation of Co nanoparticles as an additive in carbon fiber for microwave absorption enhancement in C band. *Sci Rep* 11:1–14
- [71] Han C, Zhang M, Cao WQ, Cao MS (2021) Electrospinning and in-situ hierarchical thermal treatment to tailor C-NiCo₂O₄ nanofibers for tunable microwave absorption. *Carbon* 171:953–962
- [72] Zhao B, Li Y, Ji H, Bai P, Wang S, Fan B, Guo X, Zhang R (2021) Lightweight graphene aerogels by decoration of 1D CoNi chains and CNTs to achieve ultra-wide microwave absorption. *Carbon* 176:411–420
- [73] Pawar SP, Melo G, Sundararaj U (2019) Dual functionality of hierarchical hybrid networks of multiwall carbon

- nanotubes anchored magnetite particles in soft polymer nanocomposites: Simultaneous enhancement in charge storage and microwave absorption. *Compos Sci Technol* 183:107802
- [74] Zhao PY, Wang HY, Wang GS (2020) Enhanced electromagnetic absorption properties of commercial Ni/MWCNTs composites by adjusting dielectric properties. *Front Chem* 8:97
- [75] Han T, Luo RY (2018) Effect of carbon nanotubes on the electromagnetic shielding properties of SiC_f/SiC composites. *J Alloys Compd* 745:90–99
- [76] Yu KL, Zeng M, Yin YC, Zeng XJ, Liu J, Li Y, Tang WK, Wang Y, An J, He J, Yu RH (2018) MWCNTs as conductive network for monodispersed Fe₃O₄ nanoparticles to enhance the wave absorption performances. *Adv Eng Mater* 20:1700543
- [77] Duan YP, Cui YL, Zhang B, Ma GJ, Wang TM (2019) A novel microwave absorber of FeCoNiCuAl high-entropy alloy powders: adjusting electromagnetic performance by ball milling time and annealing. *J Alloys Compd* 773:194–201
- [78] Naidu MK, Ramji K, Santhosi B, Murthy KK, Subrahmanyam C, Satyanarayana B (2018) Influence of NiFe alloy nanopowder on electromagnetic and microwave absorption properties of MWCNT/Epoxy composite. *Adv Polym Technol* 37:622–628
- [79] Yang N, Luo ZX, Zhu GR, Chen SC, Wang XL, Wu G, Wang YZ (2019) Ultralight three-dimensional hierarchical cobalt nanocrystals/N-doped CNTs/carbon sponge composites with a hollow skeleton toward superior microwave absorption. *ACS Appl Mater Interfaces* 11:35987–35998
- [80] Qiu Y, Yang HB, Ma L, Lin Y, Zong HW, Wen B, Bai XY, Wang MQ (2021) In situ-derived carbon nanotube-decorated nitrogen-doped carbon-coated nickel hybrids from MOF/melamine for efficient electromagnetic wave absorption. *J Colloid Interface Sci* 581:783–793
- [81] Zhou YL, Miao J, Shen YH, Xie AJ (2018) Novel porous Fe_xC_yN_z/N-doped CNT nanocomposites with excellent bifunctions for catalyzing oxygen reduction reaction and absorbing electromagnetic wave. *Appl Surf Sci* 453:83–92
- [82] Ning MQ, Li JB, Kuang BY, Wang CZ, Su DZ, Zhao YJ, Jin HB, Cao MS (2018) One-step fabrication of N-doped CNTs encapsulating M nanoparticles (M = Fe Co, Ni) for efficient microwave absorption. *Appl Surf Sci* 447:244–253
- [83] Yang QX, Liu L, Hui D, Chipara M (2016) Microstructure, electrical conductivity and microwave absorption properties of gamma-FeNi decorated carbon nanotube composites. *Compos Pt B-Eng* 87:256–262
- [84] Qi XS, Xu JL, Hu Q, Zhong W, Du YW (2015) Preparation, electromagnetic and enhanced microwave absorption properties of Fe nanoparticles encapsulated in carbon nanotubes. *Mater Sci Eng B-Adv Funct Solid-State Mater* 198:108–112
- [85] Wang JX, Yang JF, Yang J, Zhang H (2020) Design of a novel carbon nanotube and metal-organic framework interpenetrated structure with enhanced microwave absorption properties. *Nanotechnology* 31:394002
- [86] Yin YC, Liu XF, Wei XJ, Li Y, Nie XY, Yu RH, Shui JL (2017) Magnetically aligned Co-C/MWCNTs composite derived from MWCNT-interconnected zeolitic imidazolate frameworks for a lightweight and highly efficient electromagnetic wave absorber. *ACS Appl Mater Interfaces* 9:30850–30861
- [87] Li W, Zhang ZL, Lv YY, Wu Z, Yang L, Zou WX, Zou YH (2022) Ultralight Coral-like hierarchical Fe/CNTs/Porous carbon composite derived from biomass with tunable microwave absorption performance. *Appl Surf Sci* 571:151349
- [88] Xiao XY, Zhu WJ, Tan Z, Tian W, Guo Y, Wang H, Fu JN, Jian X (2018) Ultra-small Co/CNTs nanohybrid from metal organic framework with highly efficient microwave absorption. *Compos Pt B-Eng* 152:316–323
- [89] Wang JX, Yang JF, Yang J, Zhang H (2021) An Ni-Co bimetallic MOF-derived hierarchical CNT/CoO/Ni₂O₃ composite for electromagnetic wave absorption. *J Alloys Compd* 876:160126
- [90] Wang JX, Yang JF, Yang J, Zhang H (2020) Design of novel CNT/RGO/ZIF-8 ternary hybrid structure for lightweight and highly effective microwave absorption. *Nanotechnology* 31:414001
- [91] Dong M, Peng M, Wei W, Xu H, Liu C, Shen C (2021) Improved microwave absorption performance of double helical C/Co@CNT nanocomposite with hierarchical structures. *J Mater Chem C* 9:2178–2189
- [92] Wang L, Wen B, Bai XY, Liu C, Yang HB (2019) NiCo Alloy/carbon nanorods decorated with carbon nanotubes for microwave absorption. *ACS Appl Nano Mater* 2:7827–7838
- [93] Qiu Y, Yang H, Wen B, Ma L, Lin Y (2021) Facile synthesis of nickel/carbon nanotubes hybrid derived from metal organic framework as a lightweight, strong and efficient microwave absorber. *J Colloid Interface Sci* 590:561–570
- [94] Liu XY, Zhang X, Shen Y, Yan F, Chen YJ (2022) Fabrication of Fe/Fe₃C-nanoparticles encapsulated nitrogen-doped carbon nanotubes with thin wall thickness as high-efficiency electromagnetic wave absorbing materials. *J Alloys Compd* 898:162833
- [95] Xue W, Yang G, Bi S, Zhang JY, Hou ZL (2021) Construction of caterpillar-like hierarchically structured Co/

- MnO/CNTs derived from MnO₂/ZIF-8@ZIF-67 for electromagnetic wave absorption. *Carbon* 173:521–527
- [96] Wu F, Liu Z, Wang J, Shah T, Liu P, Zhang Q, Zhang B (2021) Template-free self-assembly of MXene and CoNi-bimetal MOF into intertwined one-dimensional heterostructure and its microwave absorbing properties. *Chem Eng J* 422:130591
- [97] Deng LL, Shu RW, Zhang JB (2022) Fabrication of ultraviolet nitrogen-doped reduced graphene oxide/nickel ferrite composite foams with three-dimensional porous network structure as ultrathin and high-performance microwave absorbers. *J Colloid Interface Sci* 614:110–119
- [98] Ghasemi A, Gordani GR, Ghasemi E (2019) Co₂W hexaferrite nanoparticles-carbon nanotube microwave absorbing nanocomposite. *J Magn Magn Mater* 469:391–397
- [99] Zhang KC, Gao XB, Zhang Q, Chen H, Chen XF (2018) Fe₃O₄ nanoparticles decorated MWCNTs@C ferrite nanocomposites and their enhanced microwave absorption properties. *J Magn Magn Mater* 452:55–63
- [100] Li YJ, Yuan MW, Liu HH, Sun GB (2020) In situ synthesis of CoFe₂O₄ nanocrystals decorated in mesoporous carbon nanofibers with enhanced electromagnetic performance. *J Alloys Compd* 826:154147
- [101] Chen J, Zheng J, Ji G (2021) Enhanced microwave absorbing ability of carbon fibers with embedded FeCo/CoFe₂O₄ nanoparticles. *ACS Appl Mater Interfaces* 13:36182–36189
- [102] Liao Z, Ma M, Tong Z, Wang R, Bi Y, Chen Y, Chung KL, Ma Y (2021) Fabrication of ZnFe₂O₄/C@PPy composites with efficient electromagnetic wave absorption properties. *J Colloid Interface Sci* 602:602–611
- [103] Pang HF, Sahu RP, Duan YP, Puri IK (2019) MnFe₂O₄-coated carbon nanotubes with enhanced microwave absorption: Effect of CNT content and hydrothermal reaction time. *Diam Relat Mat* 96:31–43
- [104] Ma J, Zhao B, Xiang H, Dai FZ, Liu Y, Zhang R, Zhou Y (2022) High-entropy spinel ferrites MFe₂O₄ (M = Mg, Mn, Fe Co, Ni, Cu, Zn) with tunable electromagnetic properties and strong microwave absorption. *J Adv Ceram* 11:754–768
- [105] Fang YH, Tang XT, Sun X, Zhang YF, Zhao JW, Yu LM, Liu Y, Zhao XL (2017) Preparation and enhanced microwave absorption properties of Ni-Co attached single-walled carbon nanotubes and CoFe₂O₄ nanocomposites. *J Appl Phys* 121:224301
- [106] Feng JT, Wang YC, Hou YH, Li JB, Li LC (2016) Synthesis and microwave absorption properties of coiled carbon nanotubes/CoFe₂O₄ composites. *Ceram Int* 42:17814–17821
- [107] Li N, Huang GW, Li YQ, Xiao HM, Feng QP, Hu N, Fu SY (2017) Enhanced microwave absorption performance of coated carbon nanotubes by optimizing the Fe₃O₄ nanocoating structure. *ACS Appl Mater Interfaces* 9:2973–2983
- [108] Shu XF, Fang B, Wu WJ, Song YA, Zhao ZJ (2021) Acicular or octahedral Fe₃O₄/rice husk-based activated carbon composites through graphitization synthesis as superior electromagnetic wave absorbers. *Compos Pt A-Appl Sci Manuf* 151:106635
- [109] Ren MM, Li FX, Wang BH, Wei JX, Yu QJ (2020) Preparation and electromagnetic wave absorption properties of carbon nanotubes loaded Fe₃O₄ composites. *J Magn Magn Mater* 513:167259
- [110] Movassagh-Alanagh F, Jalilian S, Shemshadi R, Kavianpour A (2019) Fabrication of microwave absorbing Fe₃O₄/MWCNTs@CFs nanocomposite by means of an electrophoretic co-deposition process. *Synth Met* 250:20–30
- [111] Wu GL, Jia ZR, Zhou XF, Nie GZ, Lv HL (2020) Interlayer controllable of hierarchical MWCNTs@C@Fe_xO_y cross-linked composite with wideband electromagnetic absorption performance. *Compos Pt A-Appl Sci Manuf* 128:105687
- [112] Wang YY, Song Y, Sun WJ, Dai K, Yan DX, Li ZM (2022) Highly enhanced microwave absorption for carbon nanotube/barium ferrite composite with ultra-low carbon nanotube loading. *J Mater Sci Technol* 102:115–122
- [113] Gao Y, Wang Z (2021) Microwave absorption and electromagnetic interference shielding properties of Li-Zn ferrite-carbon nanotubes composite. *J Magn Magn Mater* 528:167808
- [114] Zhao T, Jin W, Ji X, Yan H, Jiang Y, Dong Y, Yang Y, Dang A, Li H, Li T, Shang S, Zhou Z (2017) Synthesis of sandwich microstructured expanded graphite/barium ferrite connected with carbon nanotube composite and its electromagnetic wave absorbing properties. *J Alloys Compd* 712:59–68
- [115] Yin PF, Zhang LM, Sun P, Wang J, Feng X, Zhang Y, Dai JW, Tang YT (2020) Apium-derived biochar loaded with MnFe₂O₄@C for excellent low frequency electromagnetic wave absorption. *Ceram Int* 46:13641–13650
- [116] Li WX, Guo F, Wei XQ, Du YE, Chen YQ (2020) Preparation of Ni/C porous fibers derived from jute fibers for high-performance microwave absorption. *RSC Adv* 10:36644–36653
- [117] Zhao H, Cheng Y, Liu W, Yang L, Zhang B, Wang LP, Ji G, Xu ZJ (2019) Biomass-derived porous carbon-based nanostructures for microwave absorption. *Nano-Micro Lett* 11:1–17

- [118] Li WX, Qi HX, Guo F, Du Y, Song NJ, Liu YY, Chen YQ (2019) Co nanoparticles supported on cotton-based carbon fibers: A novel broadband microwave absorbent. *J Alloys Compd* 772:760–769
- [119] Yin PF, Zhang LM, Wang J, Feng X, Dai JW, Tang YT (2021) Facile preparation of cotton-derived carbon fibers loaded with hollow Fe₃O₄ and CoFe NPs for significant low-frequency electromagnetic absorption. *Powder Technol* 380:134–142
- [120] Yang ML, Yuan Y, Li Y, Sun XX, Wang SS, Liang L, Ning YH, Li JJ, Yin WL, Che RC, Li YB (2020) Dramatically enhanced electromagnetic wave absorption of hierarchical CNT/Co/C fiber derived from cotton and metal-organic-framework. *Carbon* 161:517–527
- [121] Li X, Cui EB, Xiang Z, Yu LZ, Xiong J, Pan F, Lu W (2020) Fe@NPC@CF nanocomposites derived from Fe-MOFs/biomass cotton for lightweight and high-performance electromagnetic wave absorption applications. *J Alloys Compd* 819:152952
- [122] Zhao H, Cheng Y, Ma J, Zhang Y, Ji G, Du Y (2018) A sustainable route from biomass cotton to construct lightweight and high-performance microwave absorber. *Chem Eng J* 339:432–441
- [123] Chen H, Zheng Y, Zhu X, Hong W, Tong Y, Lu Y, Pei G, Pang Y, Shen Z, Guan C (2021) Bamboo-derived porous carbons for Zn-ion hybrid supercapacitors. *Mater Res Bull* 139:111281
- [124] Perez EH, Ilunga OM, Solar DA, Gomez MCM, Bastida-Molina P (2020) Sustainable cooking based on a 3 kW air-forced multifuel gasification stove using alternative fuels obtained from agricultural wastes. *Sustainability* 12:7723
- [125] Qin Y, Ni C, Xie X, Zhang J, Wang B, Wu H, Sun X, Kimura H, Yu R, Du W (2021) Multiple reflection and scattering effects of the lotus seedpod-based activated carbon decorated with Co₃O₄ microwave absorbent. *J Colloid Interface Sci* 602:344–354
- [126] Guan HT, Wang QY, Wu XF, Pang J, Jiang ZY, Chen G, Dong CJ, Wang LH, Gong CH (2021) Biomass derived porous carbon (BPC) and their composites as lightweight and efficient microwave absorption materials. *Compos Pt B-Eng* 207:108562
- [127] Wei Y, Wang XX, Zhang JW, Liu HJ, Lv XY, Zhang MM, Liu SC, Gong CH (2017) Facile approach of Ni/C composites from Ni/cellulose composites as broadband microwave absorbing materials. *RSC Adv* 7:31129–31132
- [128] Zhang X, Dong YY, Pan F, Xiang Z, Zhu XJ, Lu W (2021) Electrostatic self-assembly construction of 2D MoS₂ wrapped hollow Fe₃O₄ nanoflowers@1D carbon tube hybrids for self-cleaning high-performance microwave absorbers. *Carbon* 177:332–343
- [129] Liu Y, Chen Z, Xie WH, Song SK, Zhang Y, Dong LJ (2019) In-Situ growth and graphitization synthesis of porous Fe₃O₄/carbon fiber composites derived from biomass as lightweight microwave absorber. *ACS Sustain Chem Eng* 7:5318–5328
- [130] Wang XL, Huang X, Chen ZR, Liao XP, Liu C, Shi B (2015) Ferromagnetic hierarchical carbon nanofiber bundles derived from natural collagen fibers: truly lightweight and high-performance microwave absorption materials. *J Mater Chem C* 3:10146–10153
- [131] Zhang T, Zhao DC, Wang LJ, Meng R, Zhao H, Zhou PY, Xia L, Zhong B, Wang HT, Wen GW (2020) A facile precursor pyrolysis route to bio-carbon/ferrite porous architecture with enhanced electromagnetic wave absorption in S-band. *J Alloys Compd* 819:153269
- [132] Fan G, Jiang Y, Xin J, Zhang Z, Fu X, Xie P, Cheng C, Liu Y, Qu Y, Sun K, Fan R (2019) Facile synthesis of Fe@Fe₃C/C nanocomposites derived from bulrush for excellent electromagnetic wave-absorbing properties. *ACS Sustain Chem Eng* 7:18765–18774
- [133] Wu F, Liu ZH, Xiu T, Zhu BL, Khan I, Liu P, Zhang QY, Zhang BL (2021) Fabrication of ultralight helical porous carbon fibers with CNTs-confined Ni nanoparticles for enhanced microwave absorption. *Compos Pt B-Eng* 215:108814
- [134] Zhao X, Yan J, Huang Y, Liu X, Ding L, Zong M, Liu P, Li T (2021) Magnetic porous CoNi@C derived from bamboo fiber combined with metal-organic-framework for enhanced electromagnetic wave absorption. *J Colloid Interface Sci* 595:78–87
- [135] Fang JY, Li P, Liu YD, Min YG (2021) Cobalt magnetic particles and carbon composite microtubes as high-performance electromagnetic wave absorbers. *J Mater Chem C* 9:2474–2482

Publisher's Note Springer Nature remains neutral with regard to jurisdictional claims in published maps and institutional affiliations.

Springer Nature or its licensor holds exclusive rights to this article under a publishing agreement with the author(s) or other rightsholder(s); author self-archiving of the accepted manuscript version of this article is solely governed by the terms of such publishing agreement and applicable law.